Mechanistic Study of the Oxidative N-Dealkylation Reactions of Bis(μ-oxo)dicopper Complexes

ARTICLE *in* JOURNAL OF THE AMERICAN CHEMICAL SOCIETY · NOVEMBER 1996

Impact Factor: 12.11 · DOI: 10.1021/ja962304k

3 AUTHORS, INCLUDING:

Samiran Mahapatra
Unilever
42 PUBLICATIONS **2,220** CITATIONS
SEE PROFILE

Jason Halfen
University of Wisconsin - Eau Claire
73 PUBLICATIONS **3,482** CITATIONS
SEE PROFILE

Mechanistic Study of the Oxidative N-Dealkylation Reactions of Bis(μ-oxo)dicopper Complexes

Samiran Mahapatra, Jason A. Halfen, and William B. Tolman*

Contribution from the Department of Chemistry and Center for Metals in Biocatalysis, University of Minnesota, 207 Pleasant St. SE, Minneapolis, Minnesota 55455

Received July 5, 1996[⊗]

Abstract: The results of experiments designed to probe the mechanism by which the bis(μ-oxo)dicopper complexes $[(LCu)_2(\mu\text{-}O)_2](ClO_4)_2$ (L = 1,4,7-tribenzyl-, 1,4,7-triisopropyl-, and 1,4-diisopropyl-7-benzyl-1,4,7-triazacyclononane ligands; L^{Bn_3}, L^{iPr_3}, and L^{iPr_2Bn}, respectively) decompose to products arising from macrocyclic ligand N-dealkylation are described. After removal of copper from the decomposed solutions, analysis of the organic products revealed N-dealkylated ligands and aldehyde or ketone, the oxygen atoms in the latter being derived from the bis(μ-oxo)-dicopper core as shown by ^{18}O-isotope labeling experiments. Thus, the overall N-dealkylation is akin to monooxygenase reactions carried out by various metalloenzymes such as cytochrome P450, dopamine β-monooxygenase, and peptidyl glycine α-amidating monooxygenase. Direct, intramolecular attack of the bis(μ-oxo)dicopper core at a ligand substituent C−H bond during the rate-determining step was indicated by the observed first-order kinetics, the results of H/D- and $^{16}O/^{18}O$-isotope and double labeling experiments, large primary kinetic deuterium isotope effects (KIEs), and Eyring activation parameters. Tunneling was implicated in the C−H bond cleavage step by the temperature dependence of the KIEs. A Hammett study of the decay of suitably functionalized derivatives of L^{Bn_3} revealed a ρ value of −0.8, consistent with the diamagnetic bis(μ-oxo)dicopper core behaving as an electrophile during C−H bond scission like the active oxidant in cytochrome P450. Subsequent hydroxyl "rebound" or a concerted mechanism is then proposed to generate a carbinolamine intermediate that decomposes to secondary amine and ketone or aldehyde final products.

Introduction

Oxidation reactions that involve copper ion-promoted activation of dioxygen are wide-spread in Nature and have numerous catalytic and synthetic applications.[1] Transformations involving hydroxylation of aliphatic hydrocarbons by monooxygenase enzymes are an important class of such oxidative conversions that are of particular interest due to the their role in metabolic pathways, their environmental significance, and the inherent difficulty of the C−H bond activation process involved. Copper-containing enzymes that carry out such reactions include dopamine β-monooxygenase (DβM), which catalyzes the benzylic hydroxylation of phenylethylamines (e.g. conversion of dopamine to the neurotransmitter norepinephrin),[2] particulate methane monooxygenase (pMMO), recently proposed to utilize a multicopper cluster to convert methane to methanol,[3] and peptidyl glycine α-amidating monooxygenase (PAM), which cleaves glycine-extended peptides in an oxidative N-dealkylation process to yield important hormonal peptides.[4] In these enzymes, copper active sites of varying nuclearity and, in many instances, poorly understood structure bind and activate O_2 in the performance of their aliphatic C−H bond activation reactions. Understanding how disparate copper protein active sites and synthetic model complexes use O_2 to oxidize substrates is an important research objective,[1,5] the attainment of which has implications within the broader context of dioxygen activation and generation by metalloproteins and synthetic catalysts.

Examples of aliphatic C−H bond activation reactions in synthetic copper−dioxygen chemistry are known, but unambiguous identification of nonenzymatic *inter*molecular aliphatic hydroxylation reactions has been elusive. More commonly, appendages of ligands complexed to copper(I) ions have been oxidized upon treatment with O_2; notable examples include the

* To whom correspondence should be addressed. FAX: (612) 624-7029. E-mail: tolman@chem.umn.edu.

⊗ Abstract published in *Advance ACS Abstracts,* November 1, 1996.

(1) (a) Fox, S.; Karlin, K. D. In *Active Oxygen in Biochemistry*; Valentine, J. S., Foote, C. S., Greenberg, A., Liebman, J. F., Eds.; Blackie Academic & Professional, Chapman & Hall: Glasgow, Scotland, 1995; pp 188−231. (b) Karlin, K. D.; Tyeklár, Z.; Zuberbühler, A. D. In *Bioinorganic Catalysis*; Reedijk, J., Ed.; Marcel Dekker, Inc.: New York, 1993; pp 261−315. (c) Kitajima, N.; Moro-oka, Y. *Chem. Rev.* **1994**, *94*, 737.

(2) (a) Klinman, J. P. *Chem. Rev.*, in press. (b) Stewart, L. C.; Klinman, J. P. *Annu. Rev. Biochem.* **1988**, *57*, 551−592.

(3) (a) Semrau, J. D.; Zolandz, D.; Lindstrom, M. E.; Chan, S. I. *J. Inorg. Biochem.* **1995**, *58*, 235−244. (b) Nguyen, H.-H. T.; Shiemke, A. K.; Jacobs, S. J.; Hales, B. J.; Lindstrom, M. E.; Chan, S. I. *J. Biol. Chem.* **1994**, *269*, 14995−15005. (c) Chan, S. I.; Nguyen, H.-H. T.; Shiemke, A. K.; Lidstrom, M. E. In *Bioinorganic Chemistry of Copper*; Karlin, K. D., Tyeklár, Z., Eds.; Chapman & Hall: New York, 1993; pp 184−195.

(4) (a) Merkler, D. J.; Kulathila, R.; Francisco, W. A.; Ash, D. E.; Bell, J. *FEBS Lett.* **1995**, *366*, 165−169. (b) Eipper, B. A.; Quon, A. S. W.; Mains, R. E.; Boswell, J. S.; Blackburn, N. J. *Biochemistry* **1995**, *34*, 2857−2865. (c) Kulathila, R.; Consalvo, A. P.; Fitzpatrick, P. F.; Freeman, J. C.; Snyder, L. M.; Villafranca, J. J.; Merkler, D. J. *Arch. Biochem. Biophys.* **1994**, *311*, 191−195. (d) Merkler, D. J.; Kulathila, R.; Young, S. D.; Freeman, J.; Villafranca, J. J. In *Bioinorganic Chemistry of Copper*; Karlin, K. D., Tyeklár, Z., Eds.; Chapman & Hall: New York, 1993; pp 196−209.

(5) Solomon, E. I.; Baldwin, M. J.; Lowery, M. D. *Chem. Rev.* **1992**, *92*, 521−542.

(6) Thompson, J. S. In *Biological & Inorganic Copper Chemistry*; Karlin, K. D., Zubieta, J., Eds.; Adenine Press: New York, 1986; Vol. 2, pp 1−10.

(7) (a) Itoh, S.; Kondo, T.; Komatsu, M.; Ohshiro, Y.; Li, C.; Kanehisa, N.; Kai, Y.; Fukuzumi, S. *J. Am. Chem. Soc.* **1995**, *117*, 4714−4715. (b) Réglier, M.; Amadéi, E.; Alilou, E. H.; Eydoux, F.; Pierrot, M.; Waegell, B. In *Bioinorganic Chemistry of Copper*; Karlin, K. D., Tyeklár, Z., Eds.; Chapman & Hall: New York, 1993; pp 348−362. (c) Alilou, E. H.; Amadéi, E.; Giorgi, M.; Pierrot, M.; Réglier, M. *J. Chem. Soc., Chem. Commun.* **1993**, 549−557.

(8) Capdevielle, P.; Maumy, M. *Tetrahedron Lett.* **1991**, *32*, 3831−3834.

(9) (a) Sanyal, I.; Mahroof-Tahir, M.; Nasir, M. S.; Ghosh, P.; Cohen, B. I.; Gultneh, Y.; Cruse, R. W.; Farooq, A.; Karlin, K. D.; Liu, S.; Zubieta, J. *Inorg. Chem.* **1992**, *31*, 4322−4332. (b) Sayre, L. M.; Tang, W.; Reddy, K. V.; Nadkarni, D. In *Bioinorganic Chemistry of Copper*; Karlin, K. D., Tyeklár, Z., Eds.; Chapman & Hall: New York, 1993; pp 236−248. (c) Reddy, K. V.; Jin, S.-J.; Arora, P. K.; Sfeir, D. S.; Maloney, S. C. F.; Urbach, F. L.; Sayre, L. M. *J. Am. Chem. Soc.* **1990**, *112*, 2332−2340.

S0002-7863(96)02304-9 CCC: $12.00

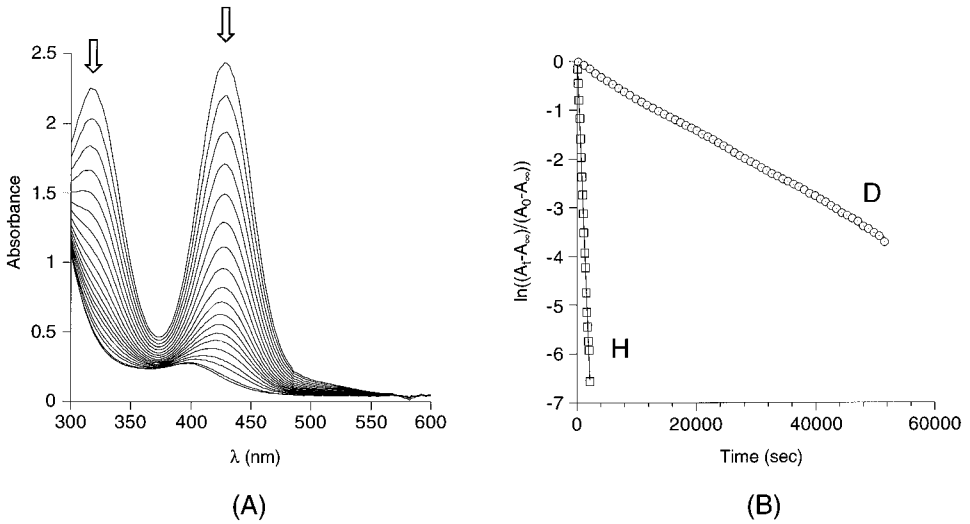

Figure 1. (A) Representative UV−vis spectral changes as a function of time for the decomposition of $[(L^{Bn_3}Cu)_2(\mu\text{-}O)_2](ClO_4)_2$ in CH_2Cl_2. (B) Representative first-order kinetics plot for the decomposition of $[(L^{Bn_3}Cu)_2(\mu\text{-}O)_2](ClO_4)_2$ (H) and $[(d_{21}\text{-}L^{Bn_3}Cu)_2(\mu\text{-}O)_2](ClO_4)_2$ (D) in CH_2Cl_2 at −40 °C. Rate constants from the slope of this plot and others are listed in Table 1.

hydroxylation of ethyl,[6] phenylethyl,[7] and amide ligand substituents[8] upon oxygenation of copper(I) complexes of N-donor ligands. Oxidative N-dealkylations (eq 1) are variants of these

$$R_2NCHR'R'' + 2H^+ + O_2 \rightarrow R_2NH + R'C(O)R'' + H_2O \quad (1)$$

reactions that also have been effected in synthetic systems[9,10] and by monooxygenases such as DβM[11] and PAM.[4,12] Mechanistic hypotheses for the various ligand oxidations invoke copper-dioxygen complexes, oxocopper species, or Cu^{III} fragments as the active oxidants, but unequivocal experimental evidence in support of the existence and/or functional role of these reactive intermediates is notably absent. As a result, there is a general lack of understanding of the fundamental C−H bond breaking event(s) inherent to the hydroxylation and N-dealkylation reactions.

We recently communicated the synthesis, characterization, and interconversion of reactive copper−dioxygen adducts having isomeric (μ-η^2:η^2-peroxo)dicopper and bis(μ-oxo)dicopper cores capped by sterically hindered *N*,*N*′,*N*″-trisubstituted 1,4,7-triazacyclononane ligands.[10,13] These compounds decompose upon warming, the latter bis(μ-oxo) compounds by N-dealkylation of the ligand substituents. In a separate full account[14] we discuss the results of experimental and theoretical studies that define the structure of the novel $[Cu_2(\mu\text{-}O)_2]^{2+}$ rhomb, as well as the $[Cu_2(\mu\text{-}OH)_2]^{2+}$ complexes capped by dealkylated macrocyclic ligands that result upon its decomposition. Here we present the outcome of an investigation aimed at shedding light on the reactivity of the bis(μ-oxo)dicopper complexes supported by 1,4,7-tribenzyl-, 1,4,7-triisopropyl-, and 1,4-diisopropyl-7-benzyl-1,4,7-triazacyclononane ligands (L^{Bn_3}, L^{iPr_3}, and L^{iPr_2Bn}, respectively) and at elucidating the mechanism of the oxidative N-dealkylations that they undergo. Through an analysis of product distributions, kinetics data, linear free energy relationships, and isotope labeling experiments, fundamental insights into the N-dealkylation pathway were obtained. On the basis of this analysis, we propose that (i) the rate-determining step involves intramolecular C−H bond scission by the intact bis(μ-oxo)dicopper core and (ii) the diamagnetic bis(μ-oxo)-dicopper core behaves like an electrophilic radical in the C−H bond activation process, much like the active oxidant in hydroxylations catalyzed by cytochrome P450.[15]

Results

Reactivity of the Bis(μ-oxo)dicopper Core with Acids and/or Ferrocene. Addition of strong protonic acids such as HBF_4·Et_2O or HO_3SCF_3 to solutions of $[(LCu)_2(\mu\text{-}O)_2](ClO_4)_2$ in CH_2Cl_2 (L = L^{Bn_3}) or THF (L = L^{iPr_3}) at −80 °C did not perturb its unique optical absorption spectrum (Figure 1A). This lack of reactivity with acids suggests that the bis(μ-oxo)dicopper core is electrophilic and contrasts with the typical behavior of oxo-bridged diiron,[16] dimanganese,[17] or mixed copper−iron complexes,[18] many of which can be protonated to yield hydroxo-bridged species. Interestingly, we previously reported[13] that the (μ-peroxo)dicopper(II) species $[(L^{iPr_3}Cu)_2(\mu\text{-}\eta^2\text{:}\eta^2\text{-}O_2)](O_3SCF_3)_2$ in CH_2Cl_2, the isomer of the L^{iPr_3}-capped bis(μ-oxo)dicopper-(III) complex, is protonated instantaneously at low temperature to ultimately yield hydrogen peroxide. The significant difference in the reactivity of the bis(oxo) and peroxo isomers with protonic acids has mechanistic implications (see the Discussion).

The bis(μ-oxo)dicopper core also can act as an outer sphere oxidant, but so far only when the redox reaction is coupled to proton transfer. Thus, no reaction was observed when $[(L^{Bn_3}Cu)_2(\mu\text{-}O)_2](ClO_4)_2$ in CH_2Cl_2 at −80 °C was treated with ferrocene, $[Cp_2Fe]$, but in the presence of HBF_4·Et_2O 2 equiv of $[Cp_2Fe]^+$ formed (Scheme 1), as shown by its distinctive

(10) (a) Mahapatra, S.; Halfen, J. A.; Wilkinson, E. C.; Pan, G.; Cramer, C. J.; Que, L., Jr.; Tolman, W. B. *J. Am. Chem. Soc.* **1995**, *117*, 8865−8866. (b) Halfen, J. A.; Mahapatra, S.; Wilkinson, E. C.; Kaderli, S.; Young, V. G., Jr.; Que, L., Jr.; Zuberbühler, A. D.; Tolman, W. B. *Science* **1996**, *271*, 1397−1400.

(11) Wimalasena, K.; May, S. W. *J. Am. Chem. Soc.* **1987**, *109*, 4036−4046.

(12) Katopodis, A. G.; May, S. W. *Biochemistry* **1990**, *29*, 4541−4548.

(13) Mahapatra, S.; Halfen, J. A.; Wilkinson, E. C.; Que, L., Jr.; Tolman, W. B. *J. Am. Chem. Soc.* **1994**, *116*, 9785−9786.

(14) Mahapatra, S.; Halfen, J. A., Wilkinson, E. C.; Pan, G.; Wang, X.; Young, V. G., Jr.; Cramer, C. J.; Que, L., Jr.; Tolman, W. B. *J. Am. Chem. Soc.* **1996**, *118*, 11555.

(15) *Cytochrome P450: Structure, Mechanism, and Biochemistry*, 2nd ed.; Ortiz de Montellano, P. R., Ed.; Plenum Press: New York, 1995.

(16) (a) Que, L., Jr.; True, A. E. *Prog. Inorg. Chem.* **1990**, *38*, 97−200. (b) Kurtz, D. M., Jr. *Chem. Rev.* **1990**, *90*, 585−606.

(17) Baldwin, M. J.; Stemmler, T. L.; Riggs-Gelasco, P. J.; Kirk, M. L.; Penner-Hahn, J. E.; Pecoraro, V. L. *J. Am. Chem. Soc.* **1994**, *116*, 11349−11356.

(18) (a) Scott, M. J.; Zhang, H. H.; Lee, S. C.; Hedman, B.; Hodgson, K. O.; Holm, R. H. *J. Am. Chem. Soc.* **1995**, *117*, 568−569. (b) Fox, S.; Nanthakumar, A.; Wikström, M.; Karlin, K. D.; Blackburn, N. J. *J. Am. Chem. Soc.* **1996**, *118*, 24−34.

Scheme 1

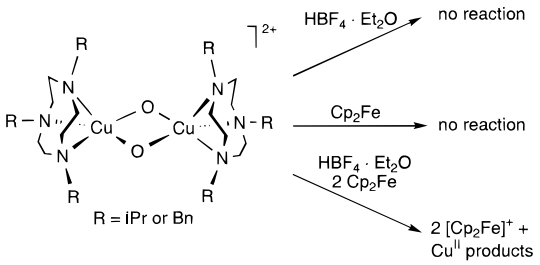

blue color, its cyclic voltammetric response, and coulometric reduction to $[Cp_2Fe]$. Monomeric copper(II)-containing compounds were generated as coproducts (overlapping axial signals in the EPR spectrum); these presumably resulted from decomposition of bis(hydroxo)dicopper(II) species by the excess acid. Because of the instability of the bis(μ-oxo)dicopper compounds, attempts to more quantitatively define their electrochemical characteristics via cyclic voltammetry, even at low temperature, have not been successful so far.

Decomposition Product Analysis. The decomposition of orange-brown solutions of $[(LCu)_2(\mu\text{-}O)_2](ClO_4)_2$ in CH_2Cl_2 ($L = L^{Bn_3}$ and L^{iPr_2Bn}) or THF ($L = L^{iPr_3}$), typically conducted after purging with N_2 to remove exogenous O_2, is accompanied by the decay of the intense optical absorption features at ∼320 and ∼430 nm characteristic for the bis(μ-oxo)dicopper core[10,14] and the concomitant growth of new features attributable to copper(II) species (Figure 1A). The predominant complexes present in the final blue-green solutions are bis(μ-hydroxo)-dicopper(II) complexes, identified as such on the basis of X-ray crystallographic characterization of isolated solids and comparison of the spectroscopic features of these solids with those of the crude product solution (e.g. UV−vis). As described elsewhere,[14] the isolated bis(μ-hydroxo)dicopper(II) complexes are capped by their respective intact macrocyclic ligands and/or N-dealkylated versions, 1,4-dibenzyl-1,4,7-triazacyclononane (L^{Bn_2H}) or 1,4-diisopropyl-1,4,7-triazacyclononane (L^{iPr_2H}). Although we cannot rule out the presence of small amounts of copper(I) products, none have been isolated, even when crystallizations were carried out under strictly anaerobic conditions.

In view of the observed variability in the yields of the various crystalline bis(μ-hydroxo)dicopper(II) products and the dependence of the nature of the products isolated on the crystallization conditions, we determined the extent of N-dealkylation by removing the copper ions and examining the organic products. This was accomplished through treatment of the decomposed solutions with aqueous NH_4OH, repetitive extraction of the organic products with CH_2Cl_2 to ensure high mass recovery (generally ∼90%), and analysis by ^1H and ^{13}C NMR spectroscopy and/or coupled gas chromatography/mass spectrometry (GC/MS). For the decompositions of both the L^{iPr_3}- and L^{Bn_3}-capped complexes, 3:2 ratios of the starting and singly dealkylated ligand products were observed (Scheme 2). Acetone or benzaldehyde was identified as the respective coproduct, in a quantity equal to that of the dealkylated ligand for the benzaldehyde case by GC/MS and NMR analysis or in somewhat lower yield for the case of acetone (presumably because a basic workup was not performed, vide infra) by GC/MS and diphenylhydrazone quantitation. Since the dealkylation reaction is an overall 2-electron oxidation, and the generation of only copper(II)-containing products from the formally bis(μ-oxo)dicopper(III) complexes involves a 2-electron reduction, the maximum yield of dealkylated ligand is 50%. In other words, at most only one of the two capping ligands in the bis(μ-oxo)dicopper complex can be dealkylated in the absence of additional oxidants, as illustrated by the formalized and balanced

Scheme 2

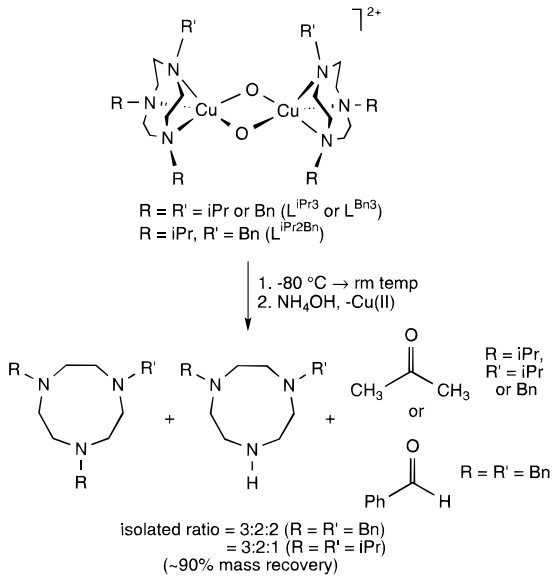

eq 2 (the addition of 1 mol of H_2O is necessary for the production of the observed bis(μ-hydroxo)dicopper(II) products). Our observation of a 3:2 ratio of unperturbed and singly dealkylated ligands with ∼90% mass recovery in reactions carried out in the absence of exogenous O_2 thus translates to ∼75% yield of isolated organic products for the dealkylation reaction.

$$R_2NCH_2R' + [Cu^{III}{}_2(O^{2-})_2]^{2+} \rightarrow R_2NH + R'CHO + [Cu^{II}{}_2(O^{2-})]^{2+} \quad (2)$$

For the case of the complex ligated by L^{iPr_2Bn} where sacrifice of either isopropyl or benzyl arms is conceivable, the predominant dealkylated ligand was that derived from isopropyl loss, 1-benzyl-4-isopropyl-1,4,7-triazacyclononane (L^{iPrHBn}); only trace amounts of L^{iPr_2H} and benzaldehyde were identified (Scheme 2). A stereoelectronic basis for the regioselectivity in this dealkylation reaction was revealed by analysis of the products obtained from the decompositions of bis(μ-oxo)-dicopper species capped by $L^{iPr_2(p-R)Bn}$, where R (CF_3 or OMe) are *para* substituents on the benzyl ring. Only isopropyl loss was observed for $L^{iPr_2(p-CF_3)Bn}$ ($R = CF_3$), but benzyl and isopropyl arm cleavage occurred to equivalent extents in the decomposition of the complex ligated by $L^{iPr_2(p-OMe)Bn}$ ($R =$ OMe). These results are consistent with the results of Hammett studies that show a rate acceleration by electron releasing substituents in the decomposition of the L^{Bn_3}-capped complex (vide infra). In the case of $L^{iPr_2(p-OMe)Bn}$, the increase in the rate of attack of the benzyl group induced by the *p*-OMe substituent is sufficiently large to affect the observed overall regioselectivity of the dealkylation process.

Kinetics. The rates of decomposition of $[(LCu)_2(\mu\text{-}O)_2](ClO_4)_2$ and analogs with perdeuterated N-substituents in CH_2Cl_2 ($L = L^{Bn_3}$ and d_{21}-L^{Bn_3}) or THF ($L = L^{iPr_3}$ and d_{21}-L^{iPr_3}) were determined as a function of temperature by monitoring the decay of the 320 and 430 nm optical absorption bands (Figure 1A). Linear ($R > 0.998$) first-order plots of $\ln[(A_t - A_\infty)/(A_0 - A_\infty)]$ versus time over greater than 4−5 half-lives yielded the rate constants (k_{obs}) listed in Table 1 (a representative first-order plot is shown in Figure 1B). Two- to three-fold decreases in the concentration of the bis(μ-oxo)dicopper complex concentrations at selected temperatures did not affect the associated rate constants, further corroborating the first-order

Table 1. Measured First-Order Rate Constants for the Decomposition of the Bis(μ-oxo)dicopper Complexes

	rate constant (s^{-1})[a]			rate constant (s^{-1})[b]	
temp (K)	L^{Bn_3}	d_{21}-L^{Bn_3}	temp (K)	L^{iPr_3}	d_{21}-L^{iPr_3}
213	$2.14(4) \times 10^{-4}$		215	$1.98(4) \times 10^{-4}$	
218	$5.26(4) \times 10^{-4}$		223	$5.33(5) \times 10^{-4}$	
				$6.10(4) \times 10^{-4}$	
223	$1.11(6) \times 10^{-3}$	$2.28(4) \times 10^{-5}$	233	$2.20(6) \times 10^{-3}$	$7.33(4) \times 10^{-5}$
	$1.09(4) \times 10^{-3}$				$8.11(4) \times 10^{-5}$
	$1.01(6) \times 10^{-3}$				
225	$1.34(4) \times 10^{-3}$		236	$3.00(4) \times 10^{-3}$	
				$3.37(4) \times 10^{-3}$	
228	$1.92(4) \times 10^{-3}$	$4.56(5) \times 10^{-5}$	240	$5.88(5) \times 10^{-3}$	
	$1.85(4) \times 10^{-3}$			$5.31(4) \times 10^{-3}$	
233	$3.49(4) \times 10^{-3}$	$9.84(5) \times 10^{-5}$	243	$6.63(6) \times 10^{-3}$	$4.12(4) \times 10^{-4}$
	$3.71(5) \times 10^{-3}$			$7.90(6) \times 10^{-3}$	$4.18(4) \times 10^{-4}$
	$3.45(5) \times 10^{-3}$				
235	$5.29(6) \times 10^{-3}$		253		$1.12(4) \times 10^{-3}$
					$1.34(5) \times 10^{-3}$
					$1.20(4) \times 10^{-3}$
237	$6.65(5) \times 10^{-3}$	$1.55(3) \times 10^{-4}$	263		$3.55(4) \times 10^{-3}$
	$6.40(5) \times 10^{-3}$	$1.49(4) \times 10^{-4}$			$3.53(4) \times 10^{-3}$
243	$1.49(5) \times 10^{-2}$	$3.80(6) \times 10^{-4}$			
	$1.71(6) \times 10^{-2}$	$3.81(4) \times 10^{-4}$			
248		$7.67(6) \times 10^{-4}$			
253		$1.44(5) \times 10^{-3}$			
		$1.31(6) \times 10^{-3}$			

[a] Measured by monitoring the loss of the 430 nm band of CH_2Cl_2 solutions. [b] Measured by monitoring the loss of the 448 nm band of THF solutions.

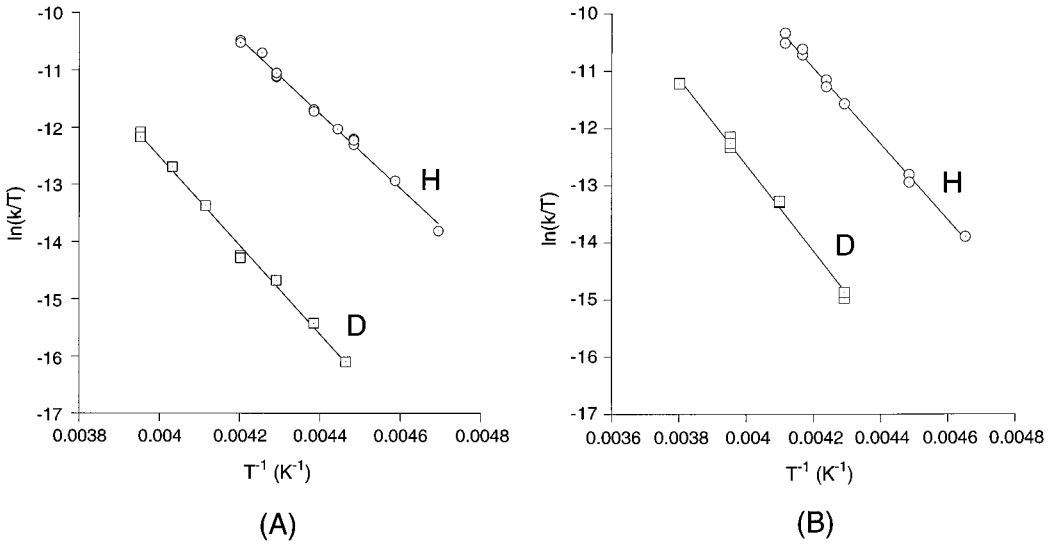

Figure 2. Eyring plots using rate constants listed in Table 1 for the decompositions of (A) $[(L^{Bn_3}Cu)_2(\mu\text{-}O)_2](ClO_4)_2$ (H) and $[(d_{21}\text{-}L^{Bn_3}Cu)_2(\mu\text{-}O)_2](ClO_4)_2$ (D) in CH_2Cl_2 and (B) $[(L^{iPr_3}Cu)_2(\mu\text{-}O)_2](ClO_4)_2$ (H) and $[(d_{21}\text{-}L^{iPr_3}Cu)_2(\mu\text{-}O)_2](ClO_4)_2$ (D) in THF.

kinetic behavior. Eyring plots of $\ln(k_{obs}T^{-1})$ versus T^{-1} (T = temperature) over ~20−40° ranges for the cases L = L^{Bn_3} and d_{21}-L^{Bn_3} in CH_2Cl_2 and L = L^{iPr_3} and d_{21}-L^{iPr_3} in THF are shown in Figure 2, with derived activation parameters listed in Table 2.

The divergent lines in Figure 1B and in the Eyring plots in Figure 2 graphically illustrate the substantial diminution of the reaction rate when the ligand substituents are perdeuterated. This effect is reflected in the differences between the calculated activation parameters for the parent ligands and those of their deuterated analogs ($\Delta\Delta H^{\ddagger}$, $\Delta\Delta S^{\ddagger}$, and the associated Arrhenius treatment values listed in Table 2). Kinetic isotope effects [KIE = $k_{obs}{}^{H}/k_{obs}{}^{D}$] calculated from the Eyring activation parameters at −40 °C are 40 ± 4 and 26 ± 2 for the L^{Bn_3} and L^{iPr_3} systems, respectively; at 20 °C they are 14 ± 1 and 12 ± 1. These large KIEs clearly indicate that ligand substituent C−H bond breaking is involved in the rate-determining step of the decomposition reaction. For the case of L^{Bn_3}, the fact that benzaldehyde is produced suggests that it is the benzylic C−H bond that is being cleaved, while the generation of acetone from L^{iPr_3} implies methine C−H bond scission. To confirm which of the isopropyl C−H bonds (methyl vs methine) in L^{iPr_3} is attacked, selectively labeled analogs having perdeuterated methyl groups (d_{18}-L^{iPr_3}) or deuterium only in the methine positions (d_3-L^{iPr_3}) were synthesized. Rate constants for the decomposition of the bis(μ-oxo)dicopper complexes of these ligands were then measured at −30 °C: $k_{obs}(d_{18}\text{-}L^{iPr_3}) = 4.82(8) \times 10^{-3}$ s^{-1} and $k_{obs}(d_3\text{-}L^{iPr_3}) = 3.48(6) \times 10^{-4}$ s^{-1}. Comparison of these values with those of the parent and perdeuterated ligand systems at −30 °C (Table 1) revealed $k_{obs}(d_{18}\text{-}L^{iPr_3}) \cong k_{obs}(L^{iPr_3})$ and $k_{obs}(d_3\text{-}L^{iPr_3}) \cong k_{obs}(d_{21}\text{-}L^{iPr_3})$, thus demonstrating that the methine C−H bond is broken selectively in the rate-determining step of the dealkylation of L^{iPr_3}.

Hammett Study. Insight into the nature of the rate-determining C−H bond breaking event in the decomposition of the benzyl-substituted system was obtained through a

Table 2. Activation Parameters for the Decomposition of the Bis(μ-oxo)dicopper Complexes

activation parameters[a,b]	$[(L^{Bn_3}Cu)_2(\mu\text{-}O)_2](ClO_4)_2$ in CH_2Cl_2	$[(L^{iPr_3}Cu)_2(\mu\text{-}O)_2](ClO_4)_2$ in THF
$\Delta H^{\ddagger}_H$, kcal mol^{-1}	13.0(5)	13.2(5)
$\Delta S^{\ddagger}_H$, eu	−13(2)	−14(2)
E_a^H, kcal mol^{-1}	13.5(5)	13.6(5)
ln(A_H)	23.4(1)	23.4(1)
$\Delta H^{\ddagger}_D$, kcal mol^{-1}	15.5(5)	15.0(5)
$\Delta S^{\ddagger}_D$, eu	−10(2)	−12(2)
E_a^D, kcal mol^{-1}	16.0(5)	15.5(5)
ln(A_D)	25.0(1)	24.1(1)
$\Delta\Delta H^{\ddagger}$, kcal mol^{-1}	−2.5	−1.8
$\Delta\Delta S^{\ddagger}$, eu	−3	−2
$E_a^H - E_a^D$, kcal mol^{-1}	−2.5	−1.9
A_H/A_D	0.20(5)	0.49(5)

[a] $\Delta H^{\ddagger}$ and $\Delta S^{\ddagger}$ values determined from plots of ln(kT^{-1}) vs T^{-1} and use of the Eyring equation $k = (RT/Nh)\exp(\Delta S^{\ddagger}/R)\exp(-\Delta H^{\ddagger}/RT)$. E_a and A values were obtained from plots of ln(k) vs T^{-1} and use of the Arrhenius equation $k = A\exp(-E_a/RT)$. [b] Superscript and subscript H and D refer to decomposition of complexes capped by protio ligand (L^{Bn_3} or L^{iPr_3}) and ligands having perdeuterated substituents (d_{21}-L^{Bn_3} or d_{21}-L^{iPr_3}), respectively.

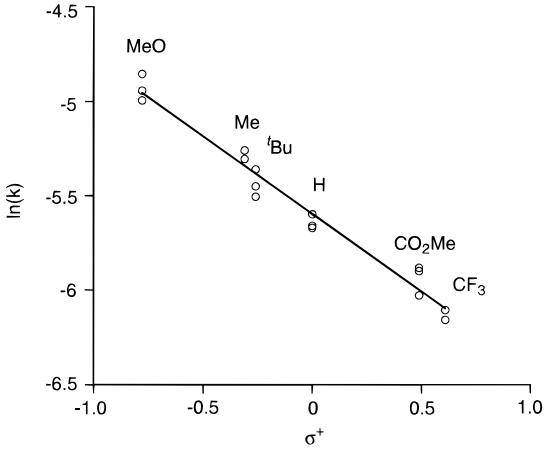

Figure 3. Hammett plot for the decomposition of $[(L^{(p-R)Bn_3}Cu)_2(\mu\text{-}O)_2](ClO_4)_2$ (R = MeO, Me, tBu, H, CO_2Me, or CF_3) in CH_2Cl_2 at −40 °C. The line represents a least squares fit to the data ($R = 0.985$), with the slope $\rho = -0.8$.

comparison of the rate constants of variants having differing *para* substituents. Copper(I) complexes of ligands $L^{(p-R)Bn_3}$ with the *para*-R-groups Me, *tert*-butyl, OMe, CF_3, and CO_2Me were prepared and reacted with O_2. The resulting species were identified as bis(μ-oxo)dicopper complexes on the basis of UV-Vis and, in the cases where R = CF_3 and OMe, ^{1}H NMR and resonance Raman spectral features that were closely analogous to those of the parent L^{Bn_3}-capped complex (data not shown). Triplicate kinetic runs for the decomposition of each in CH_2Cl_2 at −40 °C yielded rate constants which are plotted versus Hammett σ^+ values[19] in Figure 3. The good linear correlation ($R = 0.985$) supports similar transition states for the set, with the negative slope, $\rho = -0.8$, indicative of transition state stabilization by electron releasing substituents in a mechanism involving electrophilic attack at the benzylic position (see the Discussion).[20]

Isotope Labeling Experiments. Among the possible explanations for the observed first-order kinetics of the decomposition reaction is a mechanism involving a reversible pre-equilibrium between the starting bis(μ-oxo)dicopper compound

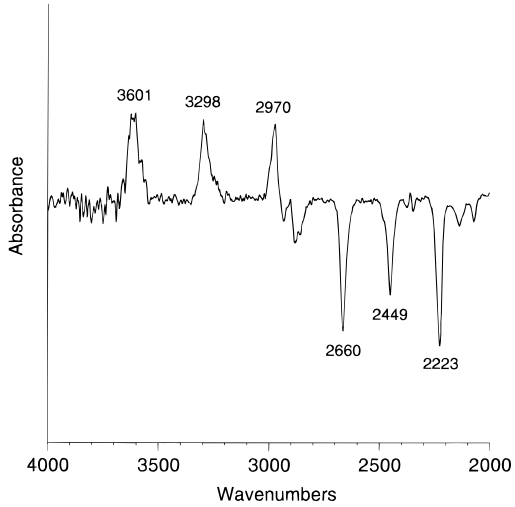

Figure 4. Difference spectrum showing the FTIR spectrum of $[(L^{iPr_2H}Cu)_2(\mu\text{-}OH)_2](ClO_4)_2$ minus that of the product derived from decomposition of $[(d_{21}\text{-}L^{iPr_3}Cu)_2(\mu\text{-}O)_2](ClO_4)_2$. See the text for peak assignments.

and monomeric $[CuO]^+$ fragments (eq 3). Such fragments have

$$[(LCu)_2(\mu\text{-}O)_2]^{2+} \rightleftharpoons 2[LCuO]^+ \qquad (3)$$

been postulated to be reactive intermediates responsible for C−H bond activation processes in both biological[2a,21] and synthetic[7b,22] systems and thus must be seriously considered as being potential culprits responsible for our oxidative dealkylation chemistry. To test for the possible intermediacy of monomeric fragments, we performed a cross-over experiment whereby equimolar solutions of $[(d_{21}\text{-}L^{Bn_3}Cu)_2(\mu\text{-}O)_2](ClO_4)_2$ in CH_2Cl_2 and $[(d_{21}\text{-}L^{iPr_3}Cu)_2(\mu\text{-}O)_2](ClO_4)_2$ in THF were mixed at −80 °C. The resulting solution was briefly warmed to −40 °C and then analyzed by electrospray ionization mass spectrometry.[23] If the bis(μ-oxo)dicopper complexes equilibrated with discrete monocopper fragments, then cross-over would be anticipated to result in the observation of a parent ion envelope corresponding to the mixed ligand complex $[(d_{21}\text{-}L^{Bn_3}Cu)(d_{21}\text{-}L^{iPr_3}Cu)(\mu\text{-}O)_2](ClO_4)_2$, with m/z 955 for the $[M - ClO_4]^+$ parent ion. In the event, only $[M - ClO_4]^+$ parent ion envelopes for the two starting complexes centered at m/z 1099 and 811 were observed and there was no evidence for the presence of the mixed ligand species. This result argues against the operation of an equilibrium involving discrete monomeric intermediates such as that shown in eq 3, at least at temperatures ≤−40 °C. Note that a cross-over experiment involving analysis of the bis(μ-hydroxo)-dicopper(II) decomposition products is precluded by the tendency for these compounds to rapidly scramble, as demonstrated by the observation reported elsewhere[14] of a 1:2:1 statistical mixture of L^{Bn_3} and/or d_{21}-L^{Bn_3}-capped complexes when $[(L^{Bn_3}Cu)_2(\mu\text{-}OH)_2](SbF_6)_2$ and $[(d_{21}\text{-}L^{Bn_3}Cu)_2(\mu\text{-}OH)_2](SbF_6)_2$ were mixed.

The movement of ligand substituent hydrogen atoms during the decomposition was tracked by analyzing the products of the reaction of deuterated isotopomers. As expected, the decomposition of $[(d_{21}\text{-}L^{Bn_3}Cu)_2(\mu\text{-}O)_2](ClO_4)_2$ only produced perdeuterated benzaldehyde. In addition, we compared the IR spectrum (KBr) of crystalline $[(L^{iPr_2H}Cu)_2(\mu\text{-}OH)_2](ClO_4)_2$ derived from $[(L^{iPr_3}Cu)_2(\mu\text{-}O)_2](ClO_4)_2$ with that of the analog derived from $[(d_{21}\text{-}L^{iPr_3}Cu)_2(\mu\text{-}O)_2](ClO_4)_2$ (Figure 4). As is

(19) Hansch, C.; Leo, A.; Taft, R. W. *Chem. Rev.* **1991**, *91*, 165−195.
(20) Johnson, C. D. *The Hammett Equation*; Cambridge University Press: Cambridge, U.K., 1973.
(21) Tian, G.; Berry, J. A.; Klinman, J. P. *Biochemistry* **1994**, *33*, 226−234.
(22) Kitajima, N.; Koda, T.; Iwata, Y.; Moro-oka, Y. *J. Am. Chem. Soc.* **1990**, *112*, 8833−8839.
(23) Kim, J.; Dong, Y.; Larka, E.; Que, L., Jr. *Inorg. Chem.* **1996**, *35*, 2369−2372.

evident from this difference spectrum, the sharp O−H (3601 cm^{-1}), N−H (3298 cm^{-1}), and C−H (2970 cm^{-1}) bands in $[(L^{iPr_2H}Cu)_2(\mu\text{-}OH)_2](ClO_4)_2$ shift to 2660, 2449, and 2223 cm^{-1}, respectively, in its congener. These shifts are consistent with the exclusive presence of N−D and O−D groups in the product of the decomposition of the deuterated bis(μ-oxo)dicopper complex [ν_{OH}/ν_{OD} (obs) = 1.353, (calc) = 1.374; ν_{NH}/ν_{ND} (obs) = 1.347, (calc) = 1.370; ν_{CH}/ν_{CD} (obs) = 1.336, (calc) = 1.362]. In other words, the ligand substituent H/D atom ends up in the complex of the dealkylated ligand in the ligand N−H/D and μ-O−H/D positions. The likelihood of rapid exchange between these two positions under the reaction and crystallization conditions unfortunately masks potentially valuable mechanistic information; nevertheless, the observations do support abstraction of the hydrogen α to the N-donor by the bis(μ-oxo)dicopper unit.

In another set of isotope labeling experiments we attempted to monitor the fate of the bridging oxygen atoms during the dealkylation process. When $^{18}O_2$ was used to generate a solution of the bis(μ-oxo)dicopper complex that was subsequently purged with N_2 to remove exogenous $^{18}O_2$ and then allowed to decompose, primarily PhCH^{18}O was identified (75:25 PhCH^{18}O/PhCH^{16}O). These results confirm that in the decomposition of $[(L^{Bn_3}Cu)_2(\mu\text{-}O)_2](ClO_4)_2$ the benzaldehyde is derived from attack of the bis(μ-oxo)dicopper core onto the benzyl ligand substituents. In these and other isotope labeling experiments to be described below, the benzaldehyde was characterized by precipitating the copper-containing products from the crude product solutions with excess Et_2O followed by analysis of the supernatant by GC/MS. Yields of benzaldehyde (and of acetone in the decomposition of the L^{iPr_3}-capped complex) were lower when this method was used (ca. 20% vs 40% after NH_4OH treatment), suggesting that base plays a role in benzaldehyde production. Nonetheless, this method was adopted because washing out of labeled oxygen atoms occurs in the presence of H_2O.[24] Indeed, the product copper complexes appear to catalyze this oxygen isotope exchange, and we presume that the small amount of PhCH^{16}O identified in the decomposition of the ^{18}O-labeled bis(μ-oxo)dicopper complex results from reaction of PhCH^{18}O with trace amounts of H_2O present in the Et_2O (used in large excess). In support of this notion, if the Et_2O used was pretreated with a small amount of $H_2{}^{18}O$ (20 μL in 4 mL) the PhCH^{18}O/PhCH^{16}O ratio increased to 85:15. Careful drying of the Et_2O used to precipitate the copper-containing products and handling only under stringent moisture-free conditions allowed us to minimize oxygen isotope exchange, but we have been unable to completely eliminate it so far.

The above results set the stage for a double-labeling experiment undertaken to determine whether oxygen incorporation into the ligand substituent is an intra- or intermolecular process (Scheme 3). The experiment involved mixing solutions of $[(L^{Bn_3}Cu)_2(\mu\text{-}O)_2](ClO_4)_2$ and $[(L^{(p-R)Bn_3}Cu)_2(\mu\text{-}^{18}O)_2](ClO_4)_2$ (R = *tert*-butyl), allowing the mixture to decompose, and then analyzing the benzaldehydes produced. Only (*p*-*tert*-butyl)C_6H_4-CH^{18}O and C_6H_5CHO (1:1) would be produced if the reaction were intramolecular, whereas a statistical mixture comprised of these benzaldehydes plus (*p*-*tert*-butyl)C_6H_4CHO and C_6H_5-CH^{18}O in equimolar amounts would result if the oxygenation was intermolecular. In the experiment, we observed C_6H_5CHO, no $C_6H_5CH^{18}O$, and an 82:18 ratio of (*p*-*tert*-butyl)$C_6H_4CH^{18}O$ and its ^{16}O isotopomer. This latter species presumably arose via ^{16}O exchange into the ^{18}O-labeled product, an hypothesis supported by observation of a similar ratio of products (84:16) in a control experiment wherein $[(L^{(p-tBu)Bn_3}Cu)_2(\mu\text{-}^{18}O)_2](ClO_4)_2$ was decomposed by itself under otherwise identical conditions. These results clearly show that the benzaldehyde product is derived from intramolecular oxygen atom transfer from the bis-(μ-oxo)dicopper core to an appended benzyl substituent.

Scheme 3

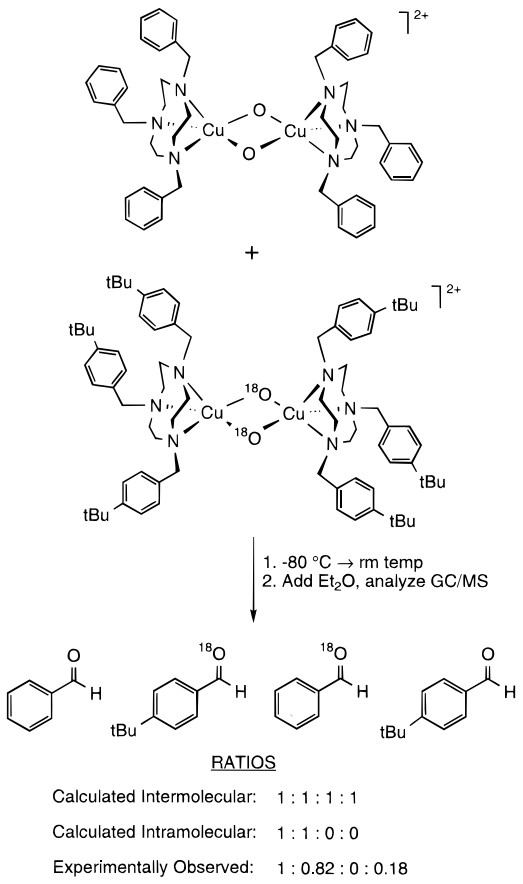

Scheme 4

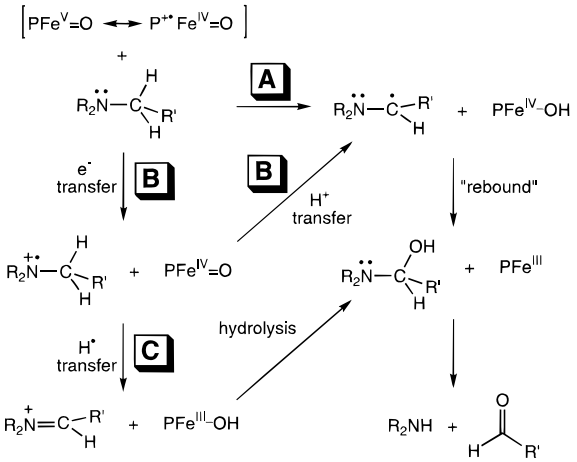

Discussion

The mechanistic framework developed to understand the N-dealkylation chemistry catalyzed by cyctochrome P450 (Scheme 4) is a reasonable starting point for our analysis of the decomposition of the bis(μ-oxo)dicopper complexes.[25] In cytochrome P450, the active oxidant is believed to be a $[FeO]^{3+}$ unit, formally $[PFe^{V}{=}O]^{+}$ or, perhaps more realistically, $[(P^{\bullet})\text{-}Fe^{IV}{=}O]^{+}$ (P = porphyrin).[26] This unit is poised to perform

(24) Bell, R. P. *Adv. Phys. Org. Chem.* **1966**, *4*, 1−29.

(25) Ortiz de Montellano, P. R. In ref 15, pp 245−303.
(26) Groves, J. T.; Han, Y.-Z. In ref 15, pp 3−48.

2-electron oxidations, which in the case of aliphatic hydrocarbon hydroxylations are generally viewed to occur via hydrogen atom abstraction followed by "rebound" of the hydroxyl group. Similarly, N-dealkylation may be initiated by hydrogen atom abstraction to yield a carbon radical α to nitrogen and $[FeOH]^{3+}$ (formally PFe^{IV}-OH, path A in Scheme 4). Alternatively, the initial step may involve electron transfer to afford an amine radical cation and $[FeO]^{2+}$ (formally PFe^{IV}═O, path B). Deprotonation of the amine radical cation would yield the same carbon radical/$[FeOH]^{3+}$ pair as generated in path A, which is envisaged to collapse to an α-hydroxylamine and $[Fe]^{3+}$. Path A thus corresponds to the classical rebound mechanism for hydrocarbon hydroxylation by cytochrome P450, with path B representing a variant potentially made accessible by the presence of the N atom. Recent arguments in favor of a nonsynchronous concerted mechanism involving "side-on" approach of $[FeO]^{3+}$ to a hydrocarbon C−H bond may be applied as a modification of path B.[27] The α-hydroxylamine also may be produced through hydrogen atom abstraction from the amine cation radical followed by hydrolysis (path C). Decomposition of the α-hydroxylamine, the intermediate common to paths A−C and one which is analogous to the usual hydroxylated products of cytochrome P450 oxidations, would then generate the final dealkylated amine and ketone or aldehyde products. The relative merits of these mechanistic postulates are discussed elsewhere;[25,28] suffice it to say here that current consensus appears to favor path B, but that ambiguities in the interpretation of experimental data remain.[29]

The drawing of an analogy between the pathways depicted in Scheme 4 and those we wish to consider for the decompositions of the bis(μ-oxo)dicopper compounds begins with the nature of the oxidant. Like the $[FeO]^{3+}$ fragment, the $[Cu_2(\mu\text{-}O)_2]^{2+}$ core, formally $[Cu^{III}_2(\mu\text{-}O^{2-})_2]^{2+}$, is disposed to act as a 2-electron oxidant, but with the oxidizing equivalents delocalized over a dimetal frame instead of a metalloporphyrin. Experimental indications of the oxidizing capabilities of the $[Cu_2(\mu\text{-}O)_2]^{2+}$ core include (i) the aforementioned proton-coupled oxidation of 2 equiv of ferrocene by $[(L^{Bn_3}Cu)_2(\mu\text{-}O)_2](ClO_4)_2$ (Scheme 1) and (ii) the generation of 2 equiv of monomeric Cu(II)−semiquinone complexes upon reaction of the bis(μ-oxo)dicopper complexes with catechols (to be reported elsewhere).[30] However, our recent finding[10b] that $[(L^{iPr_3}Cu)_2(\mu\text{-}O)_2](ClO_4)_2$ can be interconverted reversibly with its (μ-peroxo)dicopper(II) isomer $[(L^{iPr_3}Cu)_2(\mu\text{-}\eta^2\text{:}\eta^2\text{-}O_2)](ClO_4)_2$ by interchanging THF and CH_2Cl_2 solvent and that the two species coexist in a rapid equilibrium in acetone raises a potentially complicating mechanistic issue in the N-dealkylation reactions. It is conceivable that bis(μ-oxo)/peroxo equilibration also occurs in THF or CH_2Cl_2, although the lack of spectrocopic evidence for the existence of the peroxo form under the conditions described herein (for L = L^{iPr_3}, in THF; for L = L^{Bn_3} or L^{iPr_2Bn}, in any solvent) necessitates that if such an equilibrium were operative it must predominantly favor the bis(μ-oxo) form. In any case, even if the peroxo isomer is present in only small, undetectable amounts, it is possible that it is the species actually responsible for the rate-determining C−H bond cleavage step. In other words, N-dealkylation mechanisms must be considered that incorporate a rapid preequilibrium between bis(μ-oxo) and peroxo isomers, either of which may be the active oxidant. Indeed, we previously reported that $[(L^{iPr_3}Cu)_2(\mu\text{-}\eta^2\text{:}\eta^2\text{-}O_2)](O_3SCF_3)_2$ in CH_2Cl_2 decomposes to bis(μ-hydroxo)dicopper(II) complexes by a first-order process characterized by a large primary deuterium kinetic isotope effect, a result that supports isopropyl substituent C−H bond scission during the rate-controlling step.[13] The viability of the (μ-peroxo)dicopper(II) unit in oxidative chemistry is further supported by our observation of quantitivate phenol coupling via phenoxyl radical intermediates by $[(L^{iPr_3}Cu)_2(\mu\text{-}\eta^2\text{:}\eta^2\text{-}O_2)](O_3SCF_3)_2$, as well as the efficient formation of copper(II)−semiquinone complexes upon treatment of the complex with catechols.[30]

Several pieces of evidence suggest that the oxidation pathways traversed by the bis(μ-oxo) and peroxo isomers differ, however, and that under the conditions that yield the bis(μ-oxo)dicopper form exclusively as indicated by spectroscopy, equilibration with the peroxo form is not mechanistically significant. Whereas coupling of 2,4-di-*tert*-butylphenol by the peroxo complex under an inert atmosphere (N_2) is quantitative, this radical coupling reaction is much less efficient for the bis(μ-oxo) compounds under similar conditions and only affords high yields of coupled product when exogenous O_2 is present. In addition, $[(L^{iPr_3}Cu)_2(\mu\text{-}\eta^2\text{:}\eta^2\text{-}O_2)](O_3SCF_3)_2$ in CH_2Cl_2 at −80 °C reacts instantaneously with $HBF_4{\cdot}Et_2O$ to generate H_2O_2,[13] but no reaction occurs upon identical treatment of its pure bis(μ-oxo)dicopper(III) isomer in THF. Treatment of the L^{Bn_3}-capped bis(μ-oxo) complex (whose O−O bonded peroxo isomer has yet to be observed) with $HBF_4{\cdot}Et_2O$ also gives no reaction. Furthermore, the decomposition of the (μ-peroxo)dicopper(II) complex in CH_2Cl_2 results in significantly less ligand dealkylation (<15%) than the bis(μ-oxo)dicopper(III) decay reactions reported here. The temperature dependency of the KIE for the decomposition of the peroxo complex also differs from those for the bis(μ-oxo) reactions (vide infra), further supporting the intriguing hypothesis of different reactivities for the isomeric $[Cu_2(\mu\text{-}O)_2]^{2+}$ and $[Cu_2(\mu\text{-}\eta^2\text{:}\eta^2\text{-}O_2)]^{2+}$ cores. Taken together, these results suggest that even though previously reported kinetics studies showed that the peroxo and bis(μ-oxo) isomers (for L = L^{iPr_3}) exist in a rapid equilibrium in acetone solution,[10b] such an equilibrium does not occur in pure THF solution where only the bis(μ-oxo) isomer is observed spectroscopically. Thus, a rapid preequilibrium between μ-peroxo and bis(μ-oxo) compounds prior to the rate-determining C−H bond scission, although impossible to rule out solely on the grounds of the observed first-order kinetics, is nonetheless unlikely to be important in the N-dealkylation reactions discussed here that occur under conditions in which only the bis(μ-oxo) core exists.

One must also consider whether the intact $[Cu_2(\mu\text{-}O)_2]^{2+}$ core or monomeric $[CuO]^{1+}$ units derived therefrom are the active oxidizing species in the oxidative N-dealkylation reactions. As already mentioned, $[CuO]^{1+}$ monomers have been hypothesized to be responsible for hydrocarbon oxidations in both synthetic and biological systems, although spectroscopic or structural characterization of such species have yet to be reported. The experimental data we have acquired disfavor the intermediacy of a monocopper oxidant, however, and support an intramolecular mechanism involving rate-determining C−H bond scission by the intact $[Cu_2(\mu\text{-}O)_2]^{2+}$ core. Rate-determining cleavage of the core to $[CuO]^{1+}$ units would be consistent with the observed first-order kinetics, but slow monomer generation followed by rapid dealkylation is inconsistent with the negative $\Delta S^{\ddagger}$ values and the large primary deuterium kinetic isotope effects. An alternative fast preequilibrium between dinuclear and mononuclear species (eq 3) followed by rate-determining dealkylation would exhibit first-order kinetics with significant

(27) Newcomb, M.; LeTadic-Biadatti, M. H.; Chestney, D. L.; Roberts, E. S.; Hollenberg, P. F. *J. Am. Chem. Soc.* **1995**, *117*, 12085−12091.

(28) Traylor, T. G.; Traylor, P. S. In *Active Oxygen in Biochemistry*; Valentine, J. S., Foote, C. S., Greenberg, A., Liebman, J. F., Eds.; Blackie Academic & Professional: Glasgow, 1995; Vol. 3, pp 84−187.

(29) See, for example: Dennocenzo, J. P.; Karki, S. B.; Jones, J. P. *J. Am. Chem. Soc.* **1993**, *115*, 7111−7116.

(30) Mahapatra, S.; Halfen, J. A.; Houser, R. P.; Young, V. G., Jr.; Tolman, W. B. To be submitted.

Scheme 5

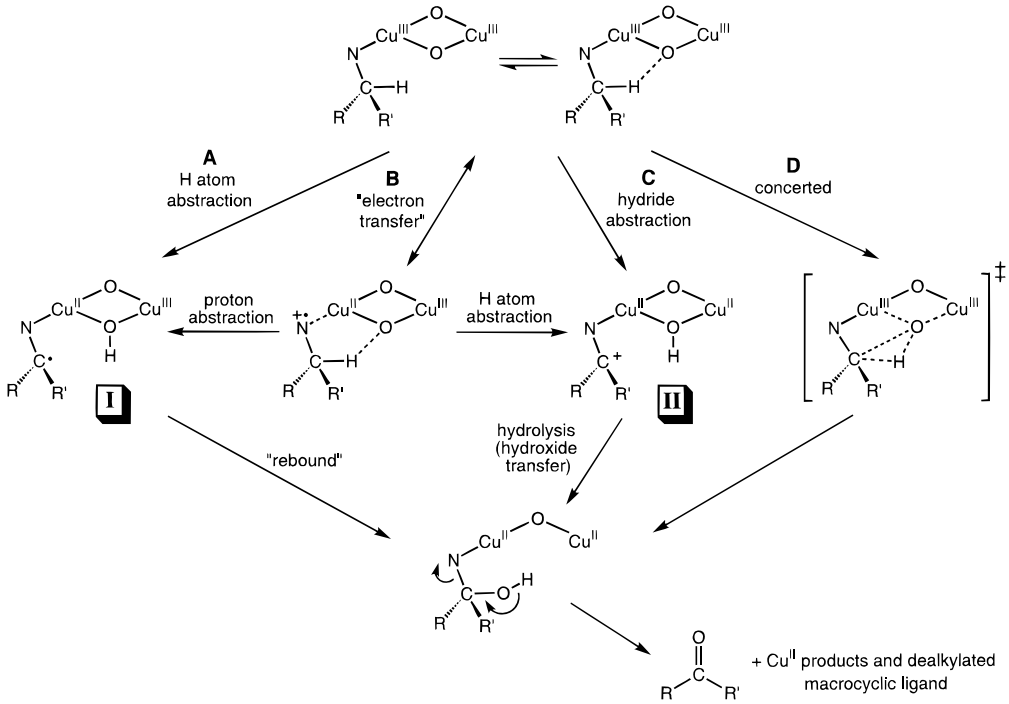

KIE values. However, this possibility is unlikely on the basis of the results of the crossover experiment which showed that mixing the d_{21}-L^{iPr_3}- and d_{21}-L^{Bn_3}-capped bis(μ-oxo)dicopper complexes did not yield the mixed ligand bis(μ-oxo)dicopper compound that would be expected to result if equilibration with discrete monomers occurred. In addition to the kinetics and crossover experiment results which argue against disruption of the bis(μ-oxo)dicopper core prior to the rate-controlling C−H bond activation step, the results of the double-labeling experiment (Scheme 3) show that the oxygen atom incorporation during the overall dealkylation process also is intramolecular.

Possible pathways consistent with the intramolecular nature of the reaction and rate-controlling C−H bond scission are presented in Scheme 5, with only one equatorial ligand N-donor and its ligand substituent (R = Ph, R′ = H or R = R′ = Me) drawn for the sake of simplicity. In view of the crystallographic results that demonstrate the existence of a C−H···O hydrogen bond between the alkyl arm and the oxo bridge,[14] we suggest that a rapid equilibrium may exist in solution between hydrogen-bonded and nonbonded forms of the bis(μ-oxo)dicopper starting material. While proof of the existence of this hydrogen bonding in solution has not been obtained, the sensitivity of the bis(μ-oxo) core vibration in resonance Raman spectra to ligand substituent deuteration[14] is certainly suggestive of this possibility. Path A is analogous to the classical cytochrome P450 rebound mechanism (path A, Scheme 4), insofar as it involves rate-determining hydrogen atom abstraction followed by fast collapse of the resulting carbon radical **I** with the hydroxyl unit (here bridging between two metal centers instead of terminally bound to a single metal ion).[26] Path B may be viewed as analogous to the electron transfer pathway B in Scheme 4, but it nonetheless is different because the amine is coordinated to copper. Thus, the coupled Cu(II)−amine radical cation is formulated as a resonance structure of the starting Cu(III)−amine rather than as a distinct intermediate. Viewing the bis-(μ-oxo)dicopper complex in this way, proton transfer would afford the same carbon-centered radical/hydroxo-bridged intermediate **I** as generated in path A. In other words, paths A and B to intermediate **I** are different formulations of the same elementary reaction step and therefore have a common transition state. Alternatively, hydrogen atom abstraction would yield a carbocation intermediate **II** (equivalent to an iminium ion) susceptible to hydrolysis via intramolecular hydroxide ion transfer. The generation of intermediate **II** may also be envisioned as a direct hydride abstraction by the dicopper(III) unit (path C). Path D is a concerted variant of path A analogous to the concerted nonsynchronous mechanism postulated for cytochrome P450 by Newcomb and co-workers.[27] In sum, there are three transition states to consider, one involving concerted attack onto the C−H bond (path D) and two others lying on the route toward intermediates **I** (radical, paths A and B) or **II** (cation, paths B and C), respectively. Each of the routes involving these three transition states involve intramolecular, rate-determining C−H bond disruption and are consistent with the observed first-order kinetics, the negative $\Delta S^{\ddagger}$ values, significant primary deuterium kinetic isotope effects (vide infra), and the isotope labeling experiments.

The results of the Hammett study (Figure 3) argue against the intermediacy of **II** (Scheme 5) but are consistent with the radical or concerted pathways. Although the ρ value (−0.8) is negative, indicating transition state stabilization by electron donating groups, it is small compared to values normally observed in reactions involving benzylic carbocation intermediates ($-5 < \rho < -2$).[20] Rather, $\rho = -0.8$ is within the range of values measured for hydrogen atom abstractions from benzylic positions by free radicals (∼0 to −1.5).[31] Similar values reported for benzylic oxidations by cytochrome P450 (−0.4)[32] and by iron porphyrin analogs [e.g., −0.8 for (TPP)-FeCl/OIPh oxidation of toluenes][33] have been interpreted to indicate that the $[FeO]^{3+}$ unit behaves as an electrophilic radical. By analogy, we favor viewing the bridging oxo group in the bis(μ-oxo)dicopper complexes as reacting like an electrophilic radical as well. Note that this does not necessarily imply a ground state structure with a high degree of radical character,

(31) Russell, G. A. In *Free Radicals*; Kochi, J. K., Ed.; John Wiley & Sons: New York, 1973; Vol. I, pp 275−331.
(32) Vaz, A. D. N.; Coon, M. J. *Biochemistry* **1994**, *33*, 6442−6449.
(33) Inchley, P.; Lindsay Smith, J. R.; Lower, R. J. *New J. Chem.* **1989**, *13*, 669−676.

a point emphasized recently by Mayer and co-workers.[34] In discussions of the mechanisms of hydrocarbon oxidations by diamagnetic oxometal reagents such as $KMnO_4$ or CrO_2Cl_2 they stressed that the rate of hydrogen atom abstraction by these reagents correlates with the O−H bond strength in the product and does not reflect radical character at the abstracting oxygen atom. Extension of this argument to our system would appear to be reasonable in view of the combined evidence in favor of a closed-shell singlet ground-state for the bis(μ-oxo)dicopper core,[14] but without thermodynamic data for the core (e.g. redox potential or pK_a) we cannot correlate the hydrogen atom abstraction rate to the (unknown) O−H bond strength. Finally, although the ρ value appears inconsistent with a generation of intermediate **II** (Scheme 5), a concerted mechanism and one involving intermediate **I** are difficult to distinguish on the basis of the Hammett study because minimal positive charge development in the transition states for each may be envisaged.

Further mechanistic insights are potentially available by consideration of the observed primary deuterium kinetic isotope effects and their temperature dependencies (Table 2). As noted above, the KIE values are quite large: at 20 °C by extrapolation, $k_H/k_D = 12$ for L^{iPr_3} and 14 for L^{Bn_3}, values significantly greater than the theoretical maximum of ∼7 predicted for complete loss of the zero-point-energy difference associated with the C−H stretching vibration in the transition state. Possible ways to account for these large effects include invoking (i) additional slightly weakened bending frequencies in the transition state (semiclassical effect), or (ii) a tunneling contribution (quantum mechanical effect).[35] Experimental evidence most commonly cited in favor of a tunneling contribution in hydrogen transfer reactions are a large KIE, an apparent activation enthalpy difference ($\Delta\Delta H^{\ddagger} = \Delta H^{\ddagger}_D - \Delta H^{\ddagger}_H$) greater than the zero-point energy difference for the reactant C−H stretch (∼1.3 kcal mol^{-1}), and a ratio of the Arrhenius preexponential factors A_H/A_D less than 0.5.[36] According to these criteria, values of $\Delta\Delta H^{\ddagger} > 1.3$ kcal mol^{-1} and $A_H/A_D \leq 0.5$ listed in Table 2 for the decomposition of the bis(μ-oxo)dicopper complexes support tunneling in the rate-determining C−H bond cleavage reaction step. Nonlinearity of an Eyring plot is also indicative of tunneling, but observation of curvature requires data acquired over a temperature range inaccessible in our experiments.

Reinaud and Theopold similarly analyzed the attack of ligand isopropyl substituent C−H bonds by a (μ-peroxo)dicobalt complex and concluded that tunneling was involved.[37] In this case, however, a transition state in which simultaneous breaking of the O−O and two C−H bonds was proposed, the constrained nature of which was suggested in part to rationalize the observed negative entropy of activation for the reaction [$\Delta S^{\ddagger} = -12(1)$ eu]. We proposed a similar transition state geometry for the rate-determining step of the decomposition of CH_2Cl_2 solutions of $[(L^{iPr_3}Cu)_2(\mu\text{-}\eta^2\text{:}\eta^2\text{-}O_2)](O_3SCF_3)_2$, the (μ-peroxo)dicopper(II) isomer of the bis(μ-oxo)dicopper(III) complex that forms in THF. Although a large KIE of 19(1) at 20 °C (by extrapolation) was observed for the decomposition of the (μ-peroxo)dicopper(II) complex, tunneling was not indicated by the activation parameters ($\Delta\Delta H^{\ddagger} \sim 0$ kcal mol^{-1} and $A_H/A_D = \sim 6$). These and other differences between the reactivities of the peroxo and bis(μ-oxo) isomers (vide supra) suggest that their C−H bond cleavage mechanisms differ, although exactly how and why they differ remains unclear.

Large KIE values comparable to or larger than those we have found have been reported in hydrocarbon hydroxylations catalyzed by a number of metalloenzymes, including cytochrome P450,[26,38] lipoxygenase,[39] and methane monooxygenase (MMO).[40] These effects are difficult to interpret, however,[41] notwithstanding the noted potential generality of large KIEs in enzyme catalyzed hydrogen transfer reactions.[42] Values of k_H/k_D in the range 11−14 (25 °C) for cytochrome P450 hydroxylations have been suggested to indicate a relatively symmetrical, linear [FeO···H···C] transition state in a rebound mechanism,[25] but this conclusion has yet to be reconciled with the view of the reaction as a nonsynchronous, concerted process involving side-on approach of the $[FeO]^{3+}$ unit to the C−H bond.[27] A rationale for the enormous KIE of 50−100 for the hydroxylation of methane by MMO similarly is lacking,[40] in part because of the difficulties inherent in predicting such effects for some of the unusual transition state structures currently under consideration.[43] Likewise, while we can suggest that geometric constraints inherent to intramolecular C−H bond scission by the bis(μ-oxo)dicopper unit would prohibit a linear O···H···C transition state, we cannot differentiate among the various proposed pathways for the decomposition of the bis(μ-oxo)-dicopper complexes (Scheme 5) on the basis of the large KIE values. All of the transition states can be envisioned to involve close approach of the oxo atom and the hydrogen atom to be abstracted (as H^+, $H^\bullet$, or H^-), corresponding to a "narrow" potential energy barrier subject to tunneling.

Conclusion

On the basis of evidence from kinetics and isotope labeling experiments, we propose a mechanism for the decomposition of the novel bis(μ-oxo)dicopper that involves direct, intramolecular attack of the intact $[Cu_2(\mu\text{-}O)_2]^{2+}$ core at the C−H bond α to the ligating N-donor of the triazacyclononane ligand in the rate determining step. This C−H bond cleavage step is characterized by a large primary deuterium kinetic isotope effect and, for the case involving benzyl substituents, a Hammett ρ of −0.8. A significant temperature dependence for the KIE was observed which is consistent with a tunneling contribution to the reaction rate. On the basis of the similarity of the small, negative ρ value to those observed in oxidations catalyzed by cytochrome P450 and some iron porphyrins, we suggest that the bis(μ-oxo)dicopper core correspondingly behaves like an electrophilic radical (notwithstanding its diamagnetic ground-state) as it effects C−H bond scission. Also like cytochrome P450 oxidations, hydroxyl rebound or a concerted, nonsynchronous pathway results in hydroxylation at the α carbon position, here an intramoleuclar transformation that is followed by rapid dealkylation to secondary amine and ketone or aldehyde final products. The electrophilic behavior of the $[Cu_2(\mu\text{-}O)_2]^{2+}$ core may be rationalized by considering its electronic structure as

(34) (a) Cook, G. K.; Mayer, J. M. *J. Am. Chem. Soc.* **1994**, *116*, 1855−1868. (b) Gardner, K. A.; Mayer, J. M. *Science* **1995**, *269*, 1849−1851.

(35) Melander, L.; Saunders, W. H., Jr. *Reaction Rates of Isotopic Molecules*; Wiley-Interscience: New York, 1980.

(36) Kwart, H. *Acc. Chem. Res.* **1982**, *15*, 408−415.

(37) Reinaud, O. M.; Theopold, K. H. *J. Am. Chem. Soc.* **1994**, *116*, 6979−6980.

(38) (a) Hjelmeland, L. M.; Aronow, L.; Trudell, J. R. *Biochem. Biophys. Res. Commun.* **1977**, *76*, 541−549. (b) Groves, J. T.; McClusky, G. A.; White, R. E.; Coon, M. J. *Biochem. Biophys. Res. Commun.* **1978**, *81*, 154−160.

(39) Glickman, M. H.; Wiseman, J. S.; Klinman, J. P. *J. Am. Chem. Soc.* **1994**, *116*, 793−794.

(40) (a) Nesheim, J. C.; Lipscomb, J. D. *J. Inorg. Biochem.* **1995**, *59*, 369. (b) Nesheim, J. C.; Lipscomb, J. D. *Biochemistry* **1996**, *35*, 10240−10247.

(41) Large KIEs calculated for hydrogen atom abstractions by atomic oxygen have been related to those for metalloenzyme hydroxylations: Pudzianowski, A. T.; Loew, G. H. *J. Phys. Chem.* **1983**, *87*, 1081−1085.

(42) Johnson, B. J.; Park, D.-H.; Kim, K.; Plapp, B. V.; Klinman, J. P. *Biochemistry* **1993**, *32*, 5503−5507.

(43) (a) Lipscomb, J. D. *Annu. Rev. Microbiol.* **1994**, *48*, 371−399. (b) Feig, A. L.; Lippard, S. J. *Chem. Rev.* **1994**, *94*, 759−805. (c) Shteinman, A. A. *FEBS Lett.* **1995**, *362*, 5−9. (d) Que, L., Jr.; Dong, Y. *Acc. Chem. Res.* **1996**, *29*, 190−196.

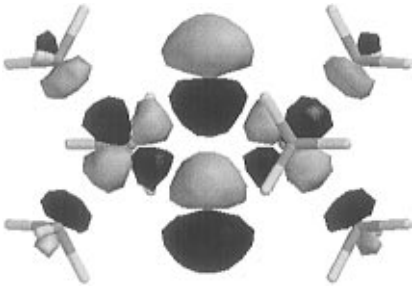

Figure 5. LUMO + 1 orbital of $\{[(NH_3)_3Cu]_2(\mu\text{-}O)_2\}^{2+}$ calculated at the RHF/STO-3G* level (0.032 bohr^{-3} isodensity surface). See ref 14.

predicted by ab initio theory.[14] We speculate that the low lying LUMO + 1 orbital (Figure 5) comprised of an antibonding combination of copper $d_{x^2-y^2}$ and oxygen p orbitals, with dominant lobes extending from the μ-O atoms, may be responsible in large part for the observed C−H bond activation reactivity.

Overall, the N-dealkylation chemistry of our synthetic system resembles the monooxygenase reactivity of cytochrome P450 and copper proteins such as DβM and PAM, although the participation of two tightly coupled copper ions in the model compounds versus the apparent involvement of only one metal center in these proteins is an important distinguishing feature. On the other hand, in a recent provocative proposal a nearby tyrosyl radical was proposed to play a role in the benzylic hydroxylation reaction catalyzed by DβM, thus bringing another oxidizing center, albeit organic, into play.[21] This and other similarities among fundamental aspects of the reactivity of the $[Cu_2(\mu\text{-}O)_2]^{2+}$, $[PFeO]^+$, and putative copper−tyrosyl radical units is consistent with an even broader conceptual relationship one may draw among various oxidized assemblies such as $[M_2(\mu\text{-}O)_2]^{n+}$ (M = Cu, Fe, or Mn, n = 2−4) units,[16a,43,44] metal-radical arrays,[45] and the mononuclear heme-iron site.[15] All of these bioinorganic functional groups reach reactive high oxidation levels by delocalizing "holes", either through sharing of charge among multiple, tightly coupled metal ions or through involvement of organic cofactors. Analysis of the structural and functional similarities and differences among these diverse, yet at least formally related species will greatly enhance our understanding of how oxidations are performed and dioxygen is utilized and generated in Nature.

Experimental Section

General Procedures. The procedures followed are described in the accompanying paper.[14] The partially deuterated reagents d_6-2-bromopropane and d_1-2-bromopropane were prepared from the appropriately deuterated 2-propanols (Cambridge) by a literature procedure.[46] Deuterium incorporation was determined by integration of the residual proton signals in the ^{1}H NMR spectra of the compounds. Low resolution electron impact mass spectra (LREIMS) were obtained on a HP GCD series G1800A GC/MS equipped with a 30 m HP-5 (crosslinked 5% PhMe-silicone) column. Helium gas was used as a carrier gas, and the flow rate was kept constant at 1.0 mL min^{-1}. The retention time t_R was measured under the following conditions: injector temperature 250 °C, initial column temperature 50 °C, duration 2.0 min, increment rate 20 °C min^{-1}, final temperautre 250 °C.

Kinetics Measurements. Low-temperature spectrophotometric studies were carried out on a Hewlett-Packard HP8452A diode array spectrophotometer (190−820 nm scan range) using a custom manufactured vacuum dewar equipped with quartz windows. To maintain and control low temperatures during kinetics studies, a copper-tubing coil was inserted into the methanol-filled UV−vis Dewar through which cold methanol was circulated from an external source (Neslab cryocool system: CC-100 II Immersion Cooler, Agitainer, and Cryotrol Temperature Controller). The temperature in the dewar was monitored by using a resistance thermocouple probe (Fluke 51 K/J Thermometer); variations over the course of kinetics runs typically were no greater than ±0.5 °C. The cuvette assembly was mounted into the dewar in the middle of the copper coil and held in place at the top with a circularly drilled Teflon plate. Before the sample was prepared, a background scan of pure solvent was taken at the particular temperature of the kinetic run.

For each kinetics run, a sample of $[LCu(CH_3CN)]ClO_4$ (∼0.002 mmol) was dissolved in 5 mL of CH_2Cl_2 (L = L^{Bn_3}) or THF (L = L^{iPr_3}) and transferred to the UV−vis cuvette assembly. The cell was placed in a methanol/liquid N_2 bath (−80 °C) and dry O_2 was bubbled through the solution until the reaction was complete (∼15 min). The cell was then transferred quickly to the methanol-filled UV−vis Dewar, which was set at the particular temperature chosen for the run. Data collection was started after equilibrating the completely immersed sample for ∼1 min at that temperature. The decomposition of the bis-(μ-oxo)dicopper complexes was followed by the intensity decrease of the characteristic charge transfer bands at 430 nm (L = L^{Bn_3}) or 448 nm (L = L^{iPr_3}). A regression analysis[47] was performed to propagate the uncertainties in the measured rate constants; additional errors in the temperature (±0.5 °C) were also considered. Activation parameters were calculated by the least-squares method from the plot of $\ln(k_{obs}T^{-1})$ versus T^{-1}.

Safety Note. ***Caution!*** *Although we have not encountered any problem, it is noted that perchlorate salts of metal complexes with organic ligands are potentially explosive and should be handled only in small quantities with appropriate precautions.*

***d*$_{18}$-L^{iPr_3} and *d*$_3$-L^{iPr_3}.** The ligands d_{18}-L^{iPr_3} and d_3-L^{iPr_3} were prepared as described in the literature using the appropriately deuterated 2-bromopropane and were isolated as clear, colorless oils. ***d*$_{18}$-L^{iPr_3}.** Deuterium content: 97% (−CH(C*D*$_3$)$_2$). ^{1}H NMR (200 MHz, CD_2Cl_2): δ 2.79 (br s, 3H) 2.59 (s, 12H) ppm. LREIMS: *m*/*z* (rel intens) 273 (1, M$^+$), 108 (100). ***d*$_3$-L^{iPr_3}.** Deuterium content: 97% (−C*D*(CH$_3$)$_2$). ^{1}H NMR (200 MHz, $CDCl_3$): δ 2.59 (s, 12H) 0.92 (br s, 18H) ppm. ^{13}C{^{1}H} NMR (75 MHz, $CDCl_3$): δ 54.0 (t, $^1J_{CD}$ = 20.1 Hz), 52.8, 18.2 ppm. LREIMS: *m*/*z* (rel intens) 258 (1, M$^+$), 102 (100).

General Method for the Synthesis of Para-Substituted Tribenzyltriazacyclononanes. To a solution of 1,4,7-triazacyclononane (0.10 g, 0.78 mmol) in toluene (∼20 mL) was added the substituted benzyl halide (3 equiv), and the mixture was refluxed for 2−3 h. Solid KOH was added to this yellow solution and the mixture was refluxed overnight. After cooling to room temperature, the reaction mixture was filtered through a Celite pad and the solvent was removed under reduced pressure to yield the products as either a thick yellow oil or a yellow solid. **1,4,7-Tris(*p*-methylbenzyl)-1,4,7-triazacyclononane (L$^{(p-Me)Bn_3}$).** Yield: 0.33 g, 97%. ^{1}H NMR ($CDCl_3$, 500 MHz): δ 7.22 (d, J = 8.0 Hz, 6H), 7.12 (d, J = 8.0 Hz, 6H), 3.57 (s, 6H), 2.80 (s, 12H), 2.35 (s, 9H) ppm. ^{13}C{^{1}H} NMR ($CDCl_3$, 125 MHz): δ 137.4, 136.2, 129.0, 128.8, 62.7, 55.3, 21.2 ppm. **1,4,7-Tris(4-*tert*-butylbenzyl)-1,4,7-triazacyclononane (L$^{(p-tBu)Bn_3}$).** Yield: 0.38 g, 86%. ^{1}H NMR ($CDCl_3$, 300 MHz): δ 7.29 (d, J = 7.0 Hz, 12H), 3.59 (s, 6H), 2.83 (s, 12H), 1.33 (s, 27H) ppm. ^{13}C{^{1}H} NMR ($CDCl_3$, 75 MHz): δ 149.5, 137.5, 128.7, 125.0, 62.6, 55.5, 34.5, 31.5 ppm. **1,4,7-Tris(*p*-methoxybenzyl)-1,4,7-triazacyclononane (L$^{(p-MeO)Bn_3}$).** Yield: 0.34 g, 90%. ^{1}H NMR ($CDCl_3$, 500 MHz): δ 7.23 (d, J = 8.5 Hz, 6H), 6.84 (d, J = 8.5 Hz, 6H), 3.80 (s, 9H), 3.53 (s, 6H), 2.77 (s, 12H) ppm. ^{13}C{^{1}H} NMR ($CDCl_3$, 125 MHz): δ 130.1, 113.4, 62.3, 55.2, 55.1 ppm. **1,4,7-Tris[*p*-(trifluoromethyl)benzyl]-1,4,7-triazacyclononane (L$^{(p-CF_3)Bn_3}$).** Yield: 0.38 g, 81%. ^{1}H NMR ($CDCl_3$, 500 MHz): δ 7.55 (d, J = 8.0 Hz, 6H), 7.43 (d, J = 8.0 Hz, 6H), 3.66 (s, 6H), 2.80 (s, 12H) ppm. ^{13}C{^{1}H} NMR ($CDCl_3$, 125 MHz): δ 144.4, 129.1, 125.1, 62.7, 55.6 ppm (CF_3 not found). **1,4,7-Tris[*p*-(car-**

(44) Manchanda, R.; Brudvig, G. W.; Crabtree, R. H. *Coord. Chem. Rev.* **1995**, *144*, 1−38.

(45) (a) Stubbe, J. A. *Annu. Rev. Biochem.* **1989**, *58*, 257−285. (b) *Metalloenzymes Involving Amino Acid Residue and Related Radicals*; Sigel, H., Sigel, A., Eds.; Marcel Dekker: New York, 1994; Vol. 30.

(46) Furness, B. S.; Hannaford, A. J.; Smith, P. W. G.; Tatchell, A. R. *Vogel's Textbook of Practical Organic Chemistry*; Longman Scientific & Technical: Essex, U.K., 1989; p 561.

(47) Skoog, D. A. *Principles of Instrumental Analysis*, 3rd ed.; Saunders College Publishing: New York, 1984; pp 5−22.

boxymethyl)benzyl]-1,4,7-triazacyclononane ($L^{(p-CO_2Me)Bn_3}$). Yield: 0.41 g, 91%. ^{1}H NMR ($CDCl_3$, 500 MHz): δ 7.97 (d, J = 8.0 Hz, 6H), 7.39 (d, J = 8.0 Hz, 6H), 3.91 (s, 9H), 3.65 (s, 6H), 2.79 (s, 12H) ppm. ^{13}C{^{1}H} NMR ($CDCl_3$, 125 MHz): δ 129.6, 128.9, 62.8, 55.6, 52.1 ppm.

1,4-Diisopropyl-7-(*p*-R-benzyl)-1,4,7-triazacyclononanes (R = CF$_3$, MeO). These ligands were synthesized in a similar manner as described for L^{iPr_2Bn}, except *p*-(trifluoromethyl)benzyl bromide or *p*-methoxybenzyl bromide was reacted with 1,4-diisopropyl-1,4,7-triazacyclononane (L^{iPr_2H}). **(R = CF$_3$; $L^{iPr_2(p-CF_3)Bn}$).** Yield: 0.51 g, 96% (based on 0.30 g (1.40 mmol) of L^{iPr_2H}). ^{1}H NMR ($CDCl_3$, 500 MHz): δ 7.52 (AB, J = 8.5 Hz, 4H), 3.71 (s, 2H), 2.92−2.86 (m, 6H), 2.62 (s, br, 8H), 0.96 (d, J = 6.5 Hz, 12H) ppm. ^{13}C{^{1}H} NMR ($CDCl_3$, 125 MHz): δ 129.0, 125.0, 61.7, 55.3, 54.8, 52.7, 52.2, 18.4 ppm. GC/MS: t_R 12.43 min, *m*/*z* (rel intens) 373 (1, M$^+$), 159 (100). **(R = MeO; $L^{iPr_2(p-MeO)Bn}$).** Yield: 0.44 g, 94% (based on 0.30 g (1.40 mmol) of L^{iPr_2H}). ^{1}H NMR ($CDCl_3$, 500 MHz): δ 7.27 (d, J = 8.5 Hz, 2H), 6.83 (d, J = 8.5 Hz, 2H), 3.79 (s, 3H), 3.59 (s, 2H), 2.92−2.84 (overlapping septet and multiplet, 6H), 2.60 (s, br, 8H), 0.95 (d, J = 6.5 Hz, 12H) ppm. ^{13}C{^{1}H} NMR ($CDCl_3$, 125 MHz): δ 130.0, 113.4, 61.5, 55.3, 55.2, 54.8, 52.7, 52.4, 18.4 ppm. GC/MS: t_R 14.27 min, *m*/*z* (rel intens) 333 (1, M$^+$), 121 (100).

[d_n-L^{iPr_3}Cu(CH$_3$CN)]ClO$_4$ (n = 18, 3). These complexes were prepared in an analogous fashion to [L^{iPr_3}Cu(CH$_3$CN)]ClO$_4$ substituting the appropriately deuterated L^{iPr_3} ligands. **[d_{18}-L^{iPr_3}Cu(CH$_3$CN)]ClO$_4$.** ^{1}H NMR (200 MHz, CD_2Cl_2): δ 3.05 (br s, 3H), 2.87−2.75 (m, 6H), 2.59−2.47 (m, 6H), 2.24 (s, 3H) ppm. **[d_3-L^{iPr_3}Cu(CH$_3$CN)]ClO$_4$.** ^{1}H NMR (300 MHz, CD_3CN): δ 2.88−2.77 (m, 6H), 2.62−2.52 (m, 6H), 1.98 (s, 3H), 1.21 (br s, 12H) ppm. ^{13}C{^{1}H} NMR (75 MHz, CD_3CN): δ 117.33, 57.21 (t,$^1J_{CD}$ 21.2 Hz), 50.46, 18.78, 0.34 ppm.

General Method for the Synthesis of [$L^{(p-R)Bn_3}$Cu(CH$_3$CN)]ClO$_4$ (R = tBu, Me, MeO, CF$_3$, and CO$_2$Me). These compounds were prepared in a manner analogous to that described for [L^{Bn_3}Cu(CH$_3$CN)]ClO$_4$ except $L^{(p-R)Bn_3}$ was used instead of L^{Bn_3}. **(R = Me).** Yield: 0.26 g, 89% (based on 0.20 g (0.45 mmol) of $L^{(p-Me)Bn_3}$). ^{1}H NMR (CD_2Cl_2, 500 MHz): δ 7.23 (d, J = 8.0 Hz, 6H), 7.12 (d, J = 8.0 Hz, 6H), 3.80 (s, 6H), 2.72−2.65 (m, 6H), 2.54−2.47 (m, 6H), 2.39 (s, 9H), 2.30 (s, br, 3H) ppm. ^{13}C{^{1}H} NMR (CD_2Cl_2, 125 MHz): δ 138.2, 131.8, 130.8, 129.0, 63.7, 52.1, 20.9 ppm. **(R = tBu).** Yield: 0.37 g, 92% (based on 0.30 g (0.53 mmol) of $L^{(p-tBu)Bn_3}$). ^{1}H NMR(CD_2Cl_2, 300 MHz): δ 7.41 (d, J = 8.1 Hz, 6H), 7.32 (d, J = 8.1 Hz, 6H), 3.85 (s, 6H), 2.73−2.64 (m, 6H), 2.54−2.44 (m, 6H), 2.39 (s, 3H), 1.36 (s, 27H) ppm. ^{13}C{^{1}H} NMR (CD_2Cl_2, 75 MHz): δ 151.5, 1331.9, 130.6, 125.3, 63.3, 51.9, 34.5, 31.3 ppm. Anal. Calcd for $C_{41}H_{60}N_4CuClO_4$: C, 63.87; H, 7.85; N, 7.27. Found: C, 63.70; H, 7.88; N, 7.24. **(R = MeO).** Yield: 0.17 g, 80% (based on 0.15 g (0.31 mmol) of $L^{(p-MeO)Bn_3}$). ^{1}H NMR (CD_2Cl_2, 300 MHz): δ 7.27 (d, J = 8.0 Hz, 6H), 6.84 (d, J = 8.0 Hz, 6H), 3.84 (s, 9H), 3.79 (s, 6H), 2.72−2.63 (m, 6H), 2.56−2.47 (m, 6H), 2.41 (s, br, 3H) ppm. ^{13}C{^{1}H} NMR (CD_2Cl_2, 75 MHz): δ 132.1, 127.0, 113.6, 63.3, 55.2, 52.1 ppm. Anal. Calcd for $C_{32}H_{45}N_4CuClO_7$: C, 55.47; H, 6.12; N, 8.09. Found: C, 55.03; H, 6.15; N, 7.97. **(R = CF$_3$).** Yield: 0.40 g, 85% (based on 0.35 g (0.58 mmol) of $L^{(p-CF_3)Bn_3}$). ^{1}H NMR (CD_2Cl_2, 300 MHz): δ 7.58−7.50 (m, 12H), 3.97 (s, 6H), 2.82−2.72 (m, 6H), 2.65−2.56 (m, 6H), 2.40 (s, 3H) ppm. ^{13}C{^{1}H} NMR (CD_2Cl_2, 75 MHz): δ 138.9, 131.5, 125.2, 63.0, 52.0 ppm. Anal. Calcd for $C_{32}H_{36}N_7CuF_9ClO_4$: C, 47.63; H, 4.13; N, 6.96. Found: C, 47.20; H, 4.17; N, 6.81. **(R = CO$_2$Me).** Yield: 0.11 g, 84% (based on 0.10 g (0.17 mmol) of $L^{(p-CO_2Me)Bn_3}$). ^{1}H NMR (CD_2Cl_2, 300 MHz): δ 7.93 (d, J = 8.1 Hz, 6H), 7.43 (d, J = 8.1 Hz, 6H), 3.95 (s, 9H), 3.92 (s, 9H) 2.78−2.68 (m, 6H), 2.64−2.55 (m, 6H), 2.43 (s, 3H) ppm. ^{13}C{^{1}H} NMR (CD_2Cl_2, 75 MHz): δ 166.4, 139.6, 131.0, 130.3, 129.4, 63.4, 52.2, 52.1 ppm. Anal. Calcd for $C_{35}H_{48}N_7CuClO_{10}$: C, 54.11; H, 5.45; N, 7.22. Found: C, 53.27; H, 5.43; N, 6.87.

[$L^{iPr_2(p-R)Bn}$Cu(CH$_3$CN)]ClO$_4$ (R = CF$_3$, MeO). These compounds were prepared in a manner analogous to that described for [L^{Bn_3}Cu(CH$_3$CN)]ClO$_4$ except $L^{iPr_2(p-R)Bn}$ was used instead of L^{Bn_3}. **(R = CF$_3$).** Yield: 0.37 g, 80% (based on 0.30 g (0.80 mmol) of $L^{iPr_2(p-CF_3)Bn}$). ^{1}H NMR (CD_2Cl_2, 300 MHz): δ 7.68 (s, 4H), 4.00 (s, 2H), 3.10−2.40 (overlapping multiplets, 14H), 2.32 (s, br, 3H), 1.19−1.14 (two overlapping doublets, J = 6.5 Hz, 12H) ppm. ^{13}C{^{1}H} NMR (CD_2Cl_2, 75 MHz): δ 131.5, 125.3, 63.6, 57.9, 51.0, 49.1, 19.8, 18.9 ppm. **(R = MeO).** Yield: 0.39 g, 81% (based on 0.30 g (0.90 mmol) of $L^{iPr_2(p-MeO)Bn}$). ^{1}H NMR (CD_2Cl_2, 500 MHz): δ 7.42 (d, J = 8.5 Hz, 4H), 6.91 (d, J = 8.5 Hz, 4H), 3.85 (s, 2H), 3.81 (s, 3H), 3.01 (septet, J = 6.5 Hz, 2H), 2.91−2.86 (m, 2H), 2.78−2.72 (m, 2H), 2.69−2.64 (m, 2H), 2.61−2.49 (m, 4H), 2.43−2.38 (m, 2H), 2.32 (s, br, 3H), 1.17 (d, J = 6.5 Hz, 6H), 1.14 (d, J = 6.5 Hz, 6H) ppm. ^{13}C{^{1}H} NMR (CD_2Cl_2, 125 MHz): δ 132.2, 127.5, 113.7, 64.0, 57.8, 55.3, 52.7, 51.1, 49.1, 19.9, 18.9 ppm.

Reaction of [(L^{Bn_3}Cu)$_2$(μ-O)$_2$](ClO$_4$)$_2$ with Ferrocene and HBF$_4$·Et$_2$O. A solution of [(L^{Bn_3}Cu)$_2$(μ-O)$_2$](ClO$_4$)$_2$ was prepared from [L^{Bn_3}Cu(CH$_3$CN)]ClO$_4$ (0.05 g, 0.08 mmol) in 10 mL of CH_2Cl_2 at −80 °C by bubbling O_2, as described elsewhere.[14] Excess O_2 was removed by bubbling N_2 through the solution for 10 min at −80 °C. A CH_2Cl_2 solution (0.5 mL) of ferrocene (0.016 g, 0.08 mmol) was added quickly to this mixture while purging the solution with N_2. No obvious color change was observed and there was no change in the UV−vis spectrum. A few drops of HBF$_4$·Et$_2$O was then introduced to the solution via syringe. The orange-brown color of the mixture immediately turned to blue. Formation of ferrocinium ion was conclusively identified from cyclic voltammetry ($E_{1/2}$ = 0.46 V (*reductive peak current*) vs SCE; ΔE_p = 80 mV) and quantified coulometrically (95% yield). An EPR spectrum of this solution contained overlapping axial copper(II) signals, presumably due to the presence of multiple mononuclear copper(II) species.

Isolation of Ligands from the Bis(μ-hydroxo)dicopper(II) Complexes: 1. L^{Bn_3} and L^{iPr_3} Ligand Systems. When an orange-brown solution of [(L^{Bn_3}Cu)$_2$(μ-O)$_2$](ClO$_4$)$_2$ (0.08 mmol) in CH_2Cl_2 (5 mL) was allowed to warm to room temperature, a blue-green solution resulted. An equal volume of concentrated aqueous ammonia was added to the blue-green solution and the mixture was stirred vigorously for few minutes giving a deep blue aqueous and a yellow CH_2Cl_2 layer. The aqueous layer was separated and further extracted with 5 mL of CH_2Cl_2. The organic extracts were combined, and the above ammonia treatment and extraction were repeated two additional times. The final CH_2Cl_2 solution was dried over $MgSO_4$ and the solvent was removed in vacuo, giving an oily yellow product. Characterization of this product by ^{1}H and ^{13}C NMR spectroscopy showed it to be a 3:2 mixture of L^{Bn_3} and L^{Bn_2H} (0.06 g, 90% mass recovery). **L^{Bn_2H}.** ^{1}H NMR ($CDCl_3$, 300 MHz): δ 7.37−7.27 (m, 10H), 3.71 (s, 4H), 2.82 (s, 4H), 2.68 (s, br, 4H), 2.56 (s, 4H) ppm. ^{13}C{^{1}H} NMR ($CDCl_3$, 75 MHz): δ 139.2, 129.5, 128.8, 127.7, 61.5, 51.6, 49.0, 45.1 ppm.

In a similar way as described above, when an orange-brown solution of [(L^{iPr_3}Cu)$_2$(μ-O)$_2$](ClO$_4$)$_2$ in THF was allowed to warm to room temperature, a green solution resulted. Following ammonia treatment to remove copper ions, organic products were analyzed by GC/MS and ^{1}H, ^{13}C NMR spectroscopy and found to be a 3:2 mixture of L^{iPr_3} and L^{iPr_2H}, respectively (90% mass recovery). GC/MS: (L^{iPr_2H}) t_R 9.47 min, *m*/*z* (rel intens) 213 (1, M$^+$), 86 (100); (L^{iPr_3}) t_R 9.97 min, *m*/*z* (rel intens) 255 (1, M$^+$), 127 (100).

2. L^{iPr_2Bn}, $L^{iPr_2(p-CF_3)Bn}$, and $L^{iPr_2(p-MeO)Bn}$ Ligand Systems. In a similar way as described above ligand isolation experiments were performed from the decomposed solutions of the bis(μ-oxo)dicopper complexes with L^{iPr_2Bn}, $L^{iPr_2(p-CF_3)Bn}$, and $L^{iPr_2(p-MeO)Bn}$ as supporting ligands. The organic products were analyzed by GC/MS and ^{1}H and ^{13}C NMR spectroscopy. For L^{iPr_2Bn} as ligand a mixture of 65% L^{iPr_2Bn}, 30% L^{iPrHBn} (minus iPr arm), 5% L^{iPr_2H} (minus Bn arm), and 5% C_6H_5-CHO was identified. **L^{iPrHBn}.** ^{1}H NMR (500 MHz, $CDCl_3$): δ 7.38−7.19 (m, 5H), 3.72 (s, 2H), 2.92−2.80 (septets, 1H), 2.70−2.42 (m, 12H), 0.97 (d, J = 6.5 Hz, 6H) ppm. ^{13}C{^{1}H} NMR ($CDCl_3$, 125 MHz): δ 142.0, 128.8, 128.1, 126.8, 61.7, 52.9, 48.5, 47.1, 46.8, 18.6 ppm. GC/MS: t_R 12.16 min, *m*/*z* (rel intens) 259 (1, M$^+$), 91 (100). **L^{iPr_2Bn}.** GC/MS: t_R 12.56 min, *m*/*z* (rel intens) 303 (5, M$^+$), 91 (100); **C_6H_5CHO.** GC/MS: t_R 5.17 min, *m*/*z* (rel intens) 106 (100, M$^+$).

For $L^{iPr_2(p-CF_3)Bn}$ as ligand, a mixture of ∼50% $L^{iPr_2(p-CF_3)Bn}$ and ∼50% $L^{iPrH(p-CF_3)Bn}$ (minus iPr arm) was identified [a peak in the GC/MS corresponsing to a trace (<1%) (*p*-CF$_3$)C$_6$H$_4$CHO was seen]. **$L^{iPrH(p-CF_3)Bn}$.** ^{1}H NMR (300 MHz, $CDCl_3$): δ 7.58−7.34 (m, 4H), 3.81 (s, 2H), 3.14−2.42 (m, 13H), 1.05 (d, J = 6.5 Hz, 6H). GC/MS: t_R 12.08 min, *m*/*z* (rel intens) 327 (1, M$^+$), 86 (100).

For $L^{iPr_2(p-MeO)Bn}$ as ligand, a mixture of 60% $L^{iPr_2(p-MeO)Bn}$, 20% $L^{iPrH(p-MeO)Bn}$ (minus iPr arm), 20% L^{iPr_2H} (minus (*p*-MeO)Bn arm), and 20% (*p*-MeO)C$_6$H$_4$CHO was identified. **$L^{iPrH(p-MeO)Bn}$.** ^{1}H NMR (300

MHz, $CDCl_3$): δ 7.28−7.24 (m, 2H), 6.84−6.81 (m, 2H), 3.88 (s, 3H), 3.64 (s, 2H), 2.92−2.82 (m, 1H), 2.60 (br, 12H), 0.95 (d, J = 6.5 Hz, 6H) ppm. GC/MS: t_R 13.73 min, *m*/*z* (rel intens) 290 (1, M^+), 121 (100). **(*p*-MeO)C$_6$H$_4$CHO.** ^{1}H NMR (300 MHz, $CDCl_3$): δ 9.88 (s, 1H), 7.83 (d, J = 8.7 Hz, 2H), 6.99 (d, J = 8.7 Hz, 2H) ppm. GC/MS: t_R 7.75 min, *m*/*z* (rel intens) 135 (100, M^+).

Crossover Experiments. A solution of $[(d_{21}\text{-}L^{Bn_3}Cu)_2(\mu\text{-}O)_2](ClO_4)_2$, prepared from oxygenation of $[d_{21}\text{-}L^{Bn_3}Cu(CH_3CN)]ClO_4$ (0.05 g, 0.08 mmol) in 5 mL of CH_2Cl_2 at −80 °C was mixed with a solution of $[(d_{21}\text{-}L^{iPr_3}Cu)_2(\mu\text{-}O)_2](ClO_4)_2$, prepared by oxygenation of $[d_{21}\text{-}L^{iPr_3}Cu(CH_3CN)]ClO_4$ (0.05 g, 0.10 mmol) in THF (5 mL) at −80 °C. After stirring for 10 min, the mixture was injected into an electrospray-MS detector using a precooled syringe at ∼−40 °C. Electrospray MS (*m*/*z* of highest peak in envelope): 1099 $[(d_{21}\text{-}L^{Bn_3}Cu)_2(\mu\text{-}O)_2(ClO_4)]^+$; 811 $[(d_{21}\text{-}L^{iPr_3}Cu)_2(\mu\text{-}O)_2(ClO_4)]^+$; no peak envelope at 955 due to $[(d_{21}\text{-}L^{iPr_3}Cu)(d_{21}\text{-}L^{Bn_3}Cu)(\mu\text{-}O)_2(ClO_4)]^+$ was observed.

Isolation of Labeled Benzaldehydes from the Decomposition of $[(d_{21}\text{-}L^{Bn_3}Cu)_2(\mu\text{-}O)_2](ClO_4)_2$ or $[(L^{Bn_3}Cu)_2(\mu\text{-}^{18}O)_2](ClO_4)_2$. Solutions of $[(d_{21}\text{-}L^{Bn_3}Cu)_2(\mu\text{-}O)_2](ClO_4)_2$ or $[(L^{Bn_3}Cu)_2(\mu\text{-}^{18}O)_2](ClO_4)_2$ in CH_2Cl_2 (10 mM) were generated at −80 °C. Exogeneous dioxygen was then removed from both flasks by bubbling N_2 for ∼10 min and the solutions were warmed to room temperature under a positive N_2 flow. The ^{18}O-labeled sample was prepared and decomposed in the presence of molecular sieves (activated, type 3A, 8−12 mesh; Baker Analyzed). Excess Et_2O was added to the resulting mixture to complete the precipitation of all copper-containing products, and the filtrate was analyzed for benzaldehyde by GC/MS. Only perdeuteriobenzaldehyde was identified for the $[(d_{21}\text{-}L^{Bn_3}Cu)_2(\mu\text{-}O)_2](ClO_4)_2$ reaction. GC/MS: t_R 5.25 min, *m*/*z* (rel intens) 112 (100, C_6D_5CDO, M^+), 110 (98, $M^+ - D$). For the reaction of $[(L^{Bn_3}Cu)_2(\mu\text{-}^{18}O)_2](ClO_4)_2$, a 3:1 ratio of $C_6H_5CH^{18}O$ [*m*/*z* 108 (100, $C_6H_5CH^{18}O$, M^+), 107 (99, $M^+ - H$)] and $C_6H_5CH^{16}O$ was observed.

Identification and Quantitation of Acetone from the Decomposition of $[(L^{iPr_3}Cu)_2(O)_2](ClO_4)_2$. 1. Identification by Mass Spectroscopy. A solution of $[(d_{21}\text{-}L^{iPr_3}Cu)_2(\mu\text{-}O)_2](ClO_4)_2$ was prepared as described elsewhere.[14] After removing excess dioxygen via three successive vacuum/N_2 cycles, the turbid orange solution was allowed to warm to room temperature under an N_2 atmosphere, resulting in the production of a green suspension. A small amount of the suspension was removed from the reaction vessel and filtered through a glass wool plug, and the filtrate was analyzed by GC/MS. d_6-Acetone was identified in the filtrate by comparison of its mass spectral pattern [*m*/*z* 64 (M^+, 28%), 46 ($M - CD_3^+$, 100%)] and GC retention time (t_R 1.52 min) to an authentic sample.

2. Quantitation by UV−Vis Spectroscopy. A solution of $[L^{iPr_3}Cu(CH_3CN)]ClO_4$ (0.052 g, 0.113 mmol) in THF (4.00 mL, [Cu] = 0.0226 M) was cooled to −80 °C and oxygenated for 1 h. After three vacuum/N_2 cycles as described above, the orange solution was warmed to room temperature. A portion of the final green suspension was filtered through glass wool, and a 0.10 mL portion of the filtrate was diluted to 10.00 mL with THF in a volumetric flask. A single drop of 2,4-dinitrophenylhydrazine reagent (prepared by dissolving 3.0 g of 2,4-dinitrophenylhydrazine in 15 mL of concentrated H_2SO_4 and then adding it to a mixture of 70 mL of EtOH and 20 mL of H_2O) was added, resulting in the production of a yellow color: λ_{max} 360 nm (A = 1.60). An acetone yield of 55% (6.2 × 10^{-4} M THF solution) was calculated by comparing the spectrum to that of an authentic, independently prepared sample of the dinitrophenylhydrazone of acetone (λ_{max} 360 nm, $\epsilon \approx 26\,000$ M^{-1} cm^{-1}).

Double-Labeling Experiment. In a Schlenk flask, solid $[L^{(p-tBu)Bn_3}Cu Cu(CH_3CN)]ClO_4$ (0.05 g, 0.065 mmol) was dissolved in 5 mL dry CH_2Cl_2, ∼20 molecular sieves (activated, type 3A, 8−12 mesh; Baker Analyzed) were added to it, and the flask was placed in a liquid N_2 bath until the solution was frozen. The headspace was evacuated on a vacuum line, excess $^{18}O_2$ was then vacuum transferred into the Schlenk flask and the flask was kept at −80 °C for ∼1 h (to ensure complete oxygenation) with occasional shaking. In a second Schlenk flask, a sample of $[(L^{Bn_3}Cu)_2(\mu\text{-}O)_2](ClO_4)_2$ was prepared by bubbling O_2 into a dry CH_2Cl_2 (5 mL) solution of $[L^{Bn_3}Cu(CH_3CN)]ClO_4$ (0.04 g, 0.066 mmol) at −80 °C in the presence of ∼20 molecular sieves. Excess dioxygen was then removed from both flasks by N_2 bubbling for ∼10 min. The two intense orange-brown solutions were then mixed quickly at −80 °C using a stainless steel cannula. After stirring for 5 min, the mixture was warmed to room temperature. Dry Et_2O (20 mL) was added to this mixture to precipitate all copper(II) species, and the organic products in the filtrate were analyzed by GC/MS: C_6H_5CHO and $C_6H_5CH^{18}O$, t_R 5.25 min, relative ratio 100:0; (*p*-tBu)$C_6H_5CH^{18}O$ and (*p*-tBu)C_6H_5CHO, t_R 8.17 min, relative ratio 82:18 [*m*/*z* (rel intens) 164 (25, (*p*-tBu)$C_6H_5CH^{18}O$, M^+), 162 (5, (*p*-tBu)C_6H_5CHO, M^+), 149 (100)]. A control experiment was also conducted in parallel, under the same conditions, in which a solution of $[(L^{(p-tBu)Bn_3}Cu)_2(\mu\text{-}^{18}O)_2](ClO_4)_2$ was allowed to decompose by itself. After precipitating the copper(II) products, GC/MS analysis of the filtrate showed a 84:16 mixture of (*p*-tBu)$C_6H_5CH^{18}O$ and (*p*-tBu)C_6H_5CHO.

Acknowledgment. We thank the National Institutes of Health (Grant GM47365), the Searle Scholars Program/Chicago Community Trust (W.B.T.), the National Science Foundation (NYI award to W.B.T.), the University of Minnesota (dissertation fellowship to J.A.H.), and the Alfred P. Sloan and Camille & Henry Dreyfus Foundations (fellowships to W.B.T.) for providing funding in support of this research. We also thank Professors John Lipscomb and Judith Klinman for providing preprints.

JA962304K